respectively. Because two mice in group A and two mice in group C died before the second period, two remaining mice in group C and one back-up mouse were assigned to group A (n=2) and group B (n=1). During the second period, mice that received high or low doses were crossed over to the alternative treatment. Serum samples were collected before the first dose was administered and 5 h after every two doses were administered. Plasma samples were also collected at the same time on days 1, 3 and 5 in the first period and days 1, 3 and 4 in the second period. The mice were sacrificed 8 h after administration of the final dose, and serum, plasma and liver samples were collected.

Experiment 5: viral kinetics with BID dosing After infection of 45 mice, 12 HCV-infected mice maintained steady-state and high viral loads (1.2×10^6–8.5×10^7 copies ml^{-1}) for more than 6 months. The median survival time of this cohort was 131 days after infection. These mice were treated with 200 mg telaprevir kg^{-1} BID at 19:00 and 9:00 h for 3 days. The mice were divided into two groups and serum samples were collected just before the second dose was administered and 4 (n=6) or 8 (n=6) h after every two doses were administered.

Serum RNA extraction and HCV RNA quantification. HCV RNA was isolated from 10 µl serum under denaturing conditions using a SepaGene RV-R kit (Sanko Junyaku). The dried precipitates were dissolved in 10 µl diethylpyrocarbonate-treated water. Extracts were duplicated and assayed by quantitative real-time RT-PCR using TaqMan EZ RT-PCR core reagents (Applied Biosystems). Nucleotide positions of the probe and primer sets refer to HCV H77 strain (GenBank accession no. AF009606). The TaqMan probe 5′-6-FAM-CTGCGGAACCGGTGAGTACAC-BHQ-1-3′ (nt 148–168) was purchased from Biosearch Technologies, and the forward (5′-CGGGAGAGCCATAGTGG-3′; nt 130–146) and reverse (5′-AGTACCACAAGGCCTTTCG-3′; nt 272–290) primers were purchased from Sigma-Aldrich. The 25 µl RT-PCR mixture contained 0.2 nmol forward and reverse primers ml^{-1}, 0.3 nmol TaqMan probe ml^{-1} and 5 µl extracted RNA, and was monitored using a PRISM 7900HT sequence detection system (Applied Biosystems). The thermal profile was 2 min at 50 °C, 30 min at 60 °C for reverse transcription and 5 min at 95 °C, followed by 45 cycles of 20 s at 95 °C and 1 min at 62 °C. The HCV replicon I_{389}neo/NS3-3′/5.1 (Lohmann *et al.*, 1999) RNA was transcribed *in vitro* using a T7 RiboMax Express Large Scale RNA Production System (Promega) and purified twice using gel filtration. The concentration of this transcribed RNA was determined by absorbance at 260 nm and serially diluted 10-fold to prepare a standard curve for each assay.

Liver RNA extraction and HCV RNA quantification. A Wizard SV total RNA Isolation System (Promega) was used to obtain a DNase I-treated total RNA sample. The total RNA concentration was determined by absorbance at 260 nm. Total RNA samples were assayed by duplex real-time RT-PCR for relative quantification of HCV RNA using endogenous control gene expression of human β_2-microglobulin (hβ_2m; GenBank accession no. NM_004048), the TaqMan probe 5′-CAL Fluor Orange 560-AGTGGGATCG-AGACATGTAAGCAGCATCAT-BHQ-1-3′ (nt 401–430), and the forward and reverse primer set of 5′-TTGTCACAGCCCAA-GATAGTT-3′ (nt 379–399) and 5′-TGCGGCATCTTCAAACC-3′ (nt 434–450). To adjust the efficacy of PCR amplification of both target genes, the reaction condition was modified from the HCV single-probe assay. The temperature for extension was 60 °C, the concentration of the HCV probe was 0.24 nmol ml^{-1} and the reaction mixture contained the TaqMan probe/primer set for hβ_2m: 0.2 nmol primers ml^{-1} and 0.12 nmol TaqMan probe ml^{-1}. Because both target genes double after one cycle of PCR, a difference in Ct between HCV and hβ2m ($\Delta Ct = Ct_{HCV} - Ct_{h\beta2m}$) theoretically indicates a relative quantity of HCV RNA per control gene expression of $2^{-\Delta\Delta Ct}$.

Determination of drug concentration. Plasma and liver samples were analysed using chiral liquid chromatography followed by tandem mass spectrometry. After reconstitution, sample extracts were separated by normal-phase chromatography on a 2 × 250 mm Hypersil CPS-1 column (Thermo Hypersil-Keystone) with a mobile phase of heptane : acetone : methanol (82 : 17 : 1). Analyte concentrations were determined by turbo ion spray liquid chromatography/tandem mass spectrometry in the positive-ion mode. Analysis was performed at SRL or Mitsubishi Chemical Medience.

Statistical analysis. The HCV RNA level in serum was normalized by logarithmic conversion. Statistical analysis was performed with a mixed linear model using SAS (SAS Institute). Mean differences between two groups were evaluated with Student's t-test. The difference compared with vehicle control at each time point was evaluated by Dunnett's multiple comparisons test. Linear and non-linear regression analyses were performed using GraphPad Prism 5 (GraphPad Software).

Viral dynamics model analysis. The basic mathematical model for the analysis of HCV infection *in vivo*, which is a system of three ordinary differential equations for uninfected cells (T), productively infected cells (I) and free virus (V), has been reviewed elsewhere (Perelson & Ribeiro, 2008). Briefly, one of the three equations ($dV/dt = pI - cV$), where viral particles are produced at rate p per infected cell and cleared at rate c per virion, was solved. During treatment for 2–3 days, if one assumes that the number of I is approximately constant and equal to its pre-treatment value and that the viral level was at its set-point value (V_0), then $pI = cV_0$. Using this relationship in the equation $dV/dt = (1-\varepsilon)pI - cV$, where ε is the effectiveness in blocking virion production, yields $dV/dt = (1-\varepsilon)\,cV_0 - cV$, $V(0) = V_0$ with the solution $V(t) = V_0(1-\varepsilon+\varepsilon e^{-ct})$. Because the log change of viral load at time [$\log \Delta V(t)$] equals $\log V(t)/V_0$, the solved equation [$\log \Delta V(t) = \log(1-\varepsilon+\varepsilon e^{-ct})$] was fitted to the values obtained in this study via non-linear least-squares regression in order to estimate ε and c.

ACKNOWLEDGEMENTS

We thank Drs Ichimaro Yamada, Mitsubishi Tanabe Pharma Corporation, and Ann D Kwong, Gururaj Kalkeri, Susan Almquist, Steven M. Lyons and John Randle, Vertex Pharmaceuticals, for their thoughtful discussions. This work was supported in part by Grants-in-Aid for scientific research and development from the Ministry of Education, Sports, Culture and Technology and the Ministry of Health, Labour and Welfare, Japan.

REFERENCES

Boonstra, A., van der Laan, L. J. W., Vanwolleghem, T., Harry, L. A. & Janssen, H. L. A. (2009). Experimental models for hepatitis C viral infection. *Hepatology* **50**, 1646–1655.

Chang, M., Williams, O., Mittler, J., Quintanilla, A., Carithers, R. L., Jr, Perkins, J., Corey, L. & Gretch, D. R. (2003). Dynamics of hepatitis C virus replication in human liver. *Am J Pathol* **163**, 433–444.

Dahari, H., Feliu, A., Garcia-Retortillo, M., Forns, X. & Neumann, A. U. (2005). Second hepatitis C replication compartment indicated by viral dynamics during liver transplantation. *J Hepatol* **42**, 491–498.

Forestier, N., Reesink, H. W., Weegink, C. J., McNair, L., Kieffer, T. L., Chu, H.-M., Purdy, S., Jansen, P. L. M. & Zeuzem, S. (2007). Antiviral

activity of telaprevir (VX-950) and peginterferon alfa-2a in patients with hepatitis C. *Hepatology* **46**, 640–648.

Fried, M. W., Shiffman, M., Reddy, K. R., Smith, C., Marinos, G., Gonçales, F. L., Jr, Häussinger, D., Diago, M., Carosi, G. & other authors (2002). Peginterferon alfa-2a plus ribavirin for chronic hepatitis C virus infection. *N Engl J Med* **347**, 975–982.

Herrmann, E., Lee, J.-H., Marinos, G., Modi, M. & Zeuzem, S. (2003). Effect of ribavirin on hepatitis C viral kinetics in patients treated with pegylated interferon. *Hepatology* **37**, 1351–1358.

Hézode, C., Forestier, N., Dusheiko, G., Ferenci, P., Pol, S., Goeser, T., Bronowicki, M., Bourlière, J.-P., Gharakhanian, S. & other authors (2009). Telaprevir and peginterferon with or without ribavirin for chronic HCV infection. *N Engl J Med* **360**, 1839–1850.

Hiraga, N., Imamura, M., Tsuge, M., Noguchi, C., Takahashi, S., Iwao, E., Fujimoto, Y., Abe, H., Maekawa, T. & other authors (2007). Infection of human hepatocyte chimeric mouse with genetically engineered hepatitis C virus and its susceptibility to interferon. *FEBS Lett* **581**, 1983–1987.

Katoh, M., Sawada, T., Soeno, Y., Nakajima, M., Tateno, C., Yoshizato, K. & Yokoi, T. (2007). *In vivo* drug metabolism model for human cytochrome P450 enzyme using chimeric mice with humanized liver. *J Pharm Sci* **96**, 428–437.

Katoh, M., Tateno, C., Yoshizato, K. & Yokoi, T. (2008). Chimeric mice with humanized liver. *Toxicology* **246**, 9–17.

Kimura, T., Imamura, M., Hiraga, N., Hatakeyama, T., Miki, D., Noguchi, C., Mori, N., Tsuge, M., Takahashi, S. & other authors (2008). Establishment of an infectious genotype 1b hepatitis C virus clone in human hepatocyte chimeric mice. *J Gen Virol* **89**, 2108–2113.

Kneteman, N. M., Weiner, A. J., O'Connell, J., Collett, M., Gao, T., Aukerman, L., Kovelsky, R., Ni, Z.-J., Hashash, A. & other authors (2006). Anti-HCV therapies in chimeric *scid*-Alb/uPA mice parallel outcomes in human clinical application. *Hepatology* **43**, 1346–1353.

Kneteman, N. M., Howe, A. Y. M., Gao, T., Lewis, J., Pevear, D., Lund, G., Douglas, D., Mercer, D. F., Tyrrell, D. L. J. & other authors (2009). HCV796: a selective nonstructural protein 5B polymerase inhibitor with potent anti-hepatitis C virus activity *in vitro*, in mice with chimeric human livers, and in humans infected with hepatitis C virus. *Hepatology* **49**, 745–752.

Lauer, G. M. & Walker, B. D. (2001). Hepatitis C virus infection. *N Engl J Med* **345**, 41–52.

Liang, T. J., Rehermann, B., Seeff, L. B. & Hoofnagle, J. H. (2000). Pathogenesis, natural history, treatment and prevention of hepatitis C. *Ann Intern Med* **132**, 296–305.

Lindenbach, B. D., Meuleman, P., Ploss, A., Vanwolleghem, T., Syder, A. J., McKeating, J. A., Lanford, R. E., Feinstone, S. M., Major, M. E. & other authors (2006). Cell culture-grown hepatitis C virus is infectious *in vivo* and can be recultured *in vitro*. *Proc Natl Acad Sci U S A* **103**, 3805–3809.

Lohmann, V., Körner, F., Koch, J., Herian, U., Theilmann, L. & Bartenschlager, R. (1999). Replication of subgenomic hepatitis C virus RNAs in a hepatoma cell line. *Science* **285**, 110–113.

Manns, M. P., McHutchison, J. G., Gordon, S. C., Rustgi, V. K., Shiffman, M., Reindollar, R., Goodman, Z. D., Koury, K., Ling, M.-H. & other authors (2001). Peginterferon alfa-2b plus ribavirin compared with interferon alfa-2b plus ribavirin for initial treatment of chronic hepatitis C: a randomised trial. *Lancet* **358**, 958–965.

Manns, M. P., Foster, G. R., Rockstroh, J. K., Zeuzem, S., Zoulim, F. & Houghton, M. (2007). The way forward in HCV treatment – finding the right path. *Nat Rev Drug Discov* **6**, 991–1000.

McHutchison, J. G., Everson, G. T., Gordon, S. C., Jacobson, I. M., Sulkowski, M., Kauffman, R., McNair, L., Alam, J., Muir, A. J. & other authors (2009). Telaprevir with peginterferon and ribavirin for chronic HCV genotype 1 infection. *N Engl J Med* **360**, 1827–1838.

Mercer, D. F., Schiller, D. E., Elliott, J. F., Douglas, D. N., Hao, C., Rinfret, A., Addison, W. R., Fischer, K. P., Churchill, T. A. & other authors (2001). Hepatitis C virus replication in mice with chimeric human livers. *Nat Med* **7**, 927–933.

Neumann, A. U., Lam, N. P., Dahari, H., Gretch, D. R., Wiley, T. E., Layden, T. J. & Perelson, A. S. (1998). Hepatitis C viral dynamics *in vivo* and the antiviral efficacy of interferon-α therapy. *Science* **282**, 103–107.

Pawlotsky, J.-M., Dahari, H., Neumann, A. U., Hezode, C., Germanidis, G., Lonjon, I., Castera, L. & Dhumeaux, D. (2004). Antiviral action of ribavirin in chronic hepatitis C. *Gastroenterology* **126**, 703–714.

Pereira, A. A. & Jacobson, I. M. (2009). New and experimental therapies for HCV. *Nat Rev Gastroenterol Hepatol* **6**, 403–411.

Perelson, A. S. & Ribeiro, R. M. (2008). Estimating drug efficacy and viral dynamic parameters: HIV and HCV. *Stat Med* **27**, 4647–4657.

Perni, R. B., Almquist, S. J., Byrn, R. A., Chandorkar, G., Chaturvedi, P. R., Courtney, L. F., Decker, C. J., Dinehart, K., Gates, C. A. & other authors (2006). Preclinical profile of VX-950, a potent, selective, and orally bioavailable inhibitor of hepatitis C virus NS3-4A serine protease. *Antimicrob Agents Chemother* **50**, 899–909.

Powers, K. A., Ribeiro, R. M., Patel, K., Pianko, S., Nyberg, L., Pockros, P., Conrad, A. J., McHutchison, J. & Perelson, A. S. (2006). Kinetics of hepatitis C virus reinfection after liver transplantation. *Liver Transpl* **12**, 207–216.

Poynard, T., Yuen, M.-F., Ratziu, V. & Lai, C. L. (2003). Viral hepatitis C. *Lancet* **362**, 2095–2100.

Quinkert, D., Bartenschlager, R. & Lohmann, V. (2005). Quantitative analysis of the hepatitis C virus replication complex. *J Virol* **79**, 13594–13605.

Ramratnam, B., Bonhoeffer, S., Binley, J., Hurley, A., Zhang, L., Mittler, J. E., Minarkowitz, M., Moore, J. P., Perelson, A. S. & Ho, D. D. (1999). Rapid production and clearance of HIV-1 and hepatitis C virus assessed by large volume plasma apheresis. *Lancet* **354**, 1782–1785.

Reesink, H. W., Zeuzem, S., Weegink, C. J., Forestier, N., Vliet, A., van de Wetering de Rooij, J., McNair, L., Purdy, S., Kauffman, R. & other authors (2006). Rapid decline of viral RNA in hepatitis C patients treated with VX-950: a phase Ib, placebo-controlled, randomized study. *Gastroenterology* **131**, 997–1002.

Sarrazin, C., Kieffer, T. L., Bartels, D., Hanzelka, B., Möh, U., Welker, M., Wincheringer, D., Zhou, Y., Chu, H.-M. & other authors (2007). Dynamic hepatitis C virus genotypic and phenotypic changes in patients treated with the protease inhibitor telaprevir. *Gastroenterology* **132**, 1767–1777.

Schiano, T. D., Gutierrez, J. A., Walewski, J. L., Fiel, M. I., Cheng, B., Bodenheimer, H., Jr, Thung, S. N., Chung, R. T., Schwartz, M. E. & other authors (2005). Accelerated hepatitis C virus kinetics but similar survival rates in recipients of liver grafts from living versus deceased donors. *Hepatology* **42**, 1420–1428.

Sherman, K. E., Fleischer, R., Laessig, K., Murray, J., Tauber, W. & Birnkrant, D. (2007). Development of novel agents for the treatment of chronic hepatitis C infection: summary of the FDA antiviral products advisory committee recommendations. *Hepatology* **46**, 2014–2020.

Talal, A. H., Ribeiro, R. M., Powers, K. A., Grace, M., Cullen, C., Hussain, M., Markatou, M. & Perelson, A. S. (2006). Pharmacodynamics of PEG-IFN α differentiate HIV/HCV coinfected sustained virological responders from nonresponders. *Hepatology* **43**, 943–953.

Tateno, C., Yoshizane, Y., Saito, N., Kataoka, M., Utoh, R., Yamasaki, C., Tachibana, A., Soeno, Y., Asahina, K. & other authors (2004). Near completely humanized liver in mice shows human-type metabolic responses to drugs. *Am J Pathol* **165**, 901–912.

Tsuge, M., Hiraga, N., Takaishi, H., Noguchi, C., Oga, H., Imamura, M., Takahashi, S., Iwao, E., Fujimoto, Y. & other authors (2005). Infection of human hepatocyte chimeric mouse with genetically engineered hepatitis B virus. *Hepatology* **42**, 1046–1054.

Vanwolleghem, T., Meuleman, P., Libbrecht, L., Roskams, T., De Vos, R. & Leroux-Roels, G. (2007). Ultra-rapid cardiotoxicity of the hepatitis C virus protease inhibitor BILN 2061 in the urokinase-type plasminogen activator mouse. *Gastroenterology* **133**, 1144–1155.

Vona, G., Tuveri, R., Delpuech, O., Vallet, A., Canioni, D., Ballardini, G., Trabut, J. B., Le Bail, B., Nalpas, B. & other authors (2004). Intrahepatic hepatitis C virus RNA quantification in microdissected hepatocytes. *J Hepatol* **40**, 682–688.

Wasley, A. & Alter, M. J. (2000). Epidemiology of hepatitis C: geographic differences and temporal trends. *Semin Liver Dis* **20**, 1–16.

Biochemical and Biophysical Research Communications 391 (2010) 316–321

Contents lists available at ScienceDirect

Biochemical and Biophysical Research Communications

journal homepage: www.elsevier.com/locate/ybbrc

Suppression of type I collagen production by microRNA-29b in cultured human stellate cells

Tomohiro Ogawa [a], Masashi Iizuka [a], Yumiko Sekiya [a,b], Katsutoshi Yoshizato [a,c], Kazuo Ikeda [d], Norifumi Kawada [a,*]

[a] Department of Hepatology, Graduate School of Medicine, Osaka City University, Osaka, Japan
[b] Toray Industries Inc., Kanagawa, Japan
[c] PhoenixBio Co. Ltd., Hiroshima, Japan
[d] Department of Functional Anatomy, Graduate School of Medicine, Nagoya City University, Aichi, Japan

ARTICLE INFO

Article history:
Received 6 November 2009
Available online 12 November 2009

Keywords:
Liver fibrosis
SP1
TGF-β
Interferon
TargetScan

ABSTRACT

MicroRNAs (miRNAs) are small noncoding RNAs that regulate gene expression through imperfect base pairing with the 3′ untranslated region (3′UTR) of target mRNA. We studied the regulation of alpha 1 (I) collagen (Col1A1) expression by miRNAs in human stellate cells, which are involved in liver fibrogenesis. Among miR-29b, -143, and -218, whose expressions were altered in response to transforming growth factor-β1 or interferon-α stimulation, miR-29b was the most effective suppressor of type I collagen at the mRNA and protein level via its direct binding to Col1A1 3′UTR. miR-29b also had an effect on SP1 expression. These results suggested that miR-29b is involved in the regulation of type I collagen expression by interferon-α in hepatic stellate cells. It is anticipated that miR-29b will be used for the regulation of stellate cell activation and lead to antifibrotic therapy.

Introduction

Hepatic stellate cells, which reside in the Disse's space outside the liver sinusoids, maintain a quiescent phenotype and store vitamin A under physiological conditions [1,2]. When liver injury occurs due to alcohol abuse, hepatitis viral infection, or obesity, stellate cells activate in response to inflammatory stimuli and become myofibroblastic cells that express smooth muscle α-actin as a representative marker [2]. Myofibroblastic cells secrete profibrogenic mediators, such as transforming growth factor-β (TGF-β), connective tissue growth factor, and tissue inhibitor of matrix metalloproteinases, and generate extracellular matrix materials including collagens, fibronectin, and laminin; thus, they play a pivotal role in liver fibrogenesis [3]. In particular, collagen production by activated stellate cells is regulated by TGF-β in an autocrine loop, which is accompanied by the induction of TGF-β receptors [4]. Suppression of hepatic stellate cell activation and collagen expression is thus a critical issue to establish therapeutic strategies for human liver fibrosis [1,5].

MicroRNAs (miRNAs) are endogenous small noncoding RNAs that modulate gene expression through imperfect base pairing with the 3′ untranslated region (UTR) of target mRNA, resulting in the inhibition of translation or the promotion of mRNA degradation [6,7]. miRNAs play roles in cell proliferation [8], development [9], and differentiation [10], and their contribution to human diseases such as cancer, cardiomyopathies, and schizophrenia have been reported [11–13]. miR-122 is also involved in the defense system against viral hepatitis C with regard to interferon (IFN)-β therapy [14], and miR-26 expression status is associated with survival and response to adjuvant IFNα therapy in patients with hepatocellular carcinoma [15]. Some miRNAs are involved in liver development and hepatocyte lipid metabolism [16–18].

Recent studies have shown that miRNAs are additionally involved in the alteration of hepatic stellate cell phenotypes; down-regulation of miR-27a and -27b allows culture-activated rat stellate cells to return to a quiescent phenotype with abundant vitamin A storage and decreased cell proliferation [19]; miR-15b and -16, which target the Bcl-2 and caspase signaling pathways, may affect stellate cell activation and liver fibrosis [20]. However, the function of miRNAs in hepatic stellate cell activation and their collagen production is largely unknown.

Here, we show that miR-29b, which is induced in human stellate cells (LX-2) treated with IFNα, is a potential regulator of type I collagen mRNA and protein expression. Although the primary action of IFNs is to eradicate viruses, i.e., hepatitis B and C viruses in

Abbreviations: Col1A1, alpha 1 (I) collagen; DMEM, Dulbecco's modified Eagle's medium; FBS, fetal bovine serum; IFN, interferon; miRNAs, microRNAs; TGF-β, transforming growth factor-β; UTR, untranslated region.

* Corresponding author. Address: Department of Hepatology, Graduate School of Medicine, Osaka City University, 1-4-3, Asahimachi, Abeno, Osaka 545-8585, Japan. Fax: +81 6 6646 9072.
E-mail address: kawadanori@med.osaka-cu.ac.jp (N. Kawada).

0006-291X/$ - see front matter © 2009 Elsevier Inc. All rights reserved.
doi:10.1016/j.bbrc.2009.11.056

the case of the liver, IFNs also exhibit an antifibrotic action in human chronic hepatitis [21,22] and rodent liver fibrosis models [23]. Our data suggest that miR-29b may be a novel regulator of type I collagen expression in addition to its involvement in the well-known Smad cascade. Moreover, miR-29b upregulation may play a partial role in the antifibrotic action of IFNs.

Materials and methods

Materials. Recombinant human TGF-β1 was purchased from PeproTech (London, UK). Human natural IFNα was obtained from Otsuka Pharmaceutical Co. (Tokushima, Japan). Precursors of miR-29b, -143, and -218, and the negative control were purchased from Ambion (Austin, TX, USA). Dulbecco's modified Eagle's medium (DMEM) and fetal bovine serum (FBS) were purchased from Sigma Chemical Co. (St. Louis, MO, USA). Rabbit monoclonal antibodies against Smad2 and phospho-Smad2 were purchased from Cell Signaling Technology Inc. (Beverly, MA, USA). The mouse monoclonal antibody against SP1 was purchased from Bio Matrix Research Inc. (Chiba, Japan). Rabbit polyclonal antibody against type I collagen was purchased from Rockland Immunochemicals, Inc. (Gilbertsville, PA, USA). Mouse monoclonal antibody against GAPDH was purchased from Chemicon International Inc. (Temecula, CA, USA). Enhanced Chemiluminescence plus detection reagent was purchased from GE Healthcare (Buckinghamshire, UK). Immobilon P membranes were purchased from Millipore Corp. (Bedford, MA, USA). All other reagents were purchased from Sigma Chemical Co. or Wako Pure Chemical Co. (Osaka, Japan).

Preparation of the human hepatic stellate cell line LX-2. The human hepatic stellate cell line (LX-2, donated by Dr. Scott Friedman), which was spontaneously immortalized by growth in low serum, was established as reported previously [24]. Characterizations of the cells are described in detail elsewhere. The cells were maintained on plastic culture plates in DMEM supplemented with 10% FBS. After the culture had continued for the indicated number of days, the medium was replaced with DMEM supplemented with 0.1% FBS plus test agents, and the culture was continued for another 24 h.

Quantitative real-time PCR. Total RNA was extracted from human stellate cells using the miRNeasy Mini Kit (Qiagen, Valencia, CA, USA). cDNAs were synthesized using 0.5 μg of total RNA, ReverTra Ace (Toyobo, Osaka, Japan), and oligo(dT)$_{12-18}$ primers according to the manufacturer's instructions [25]. Gene expression was measured by real-time PCR using cDNA, real-time PCR Master Mix Reagents (Toyobo), and a set of gene-specific oligonucleotide primers (alpha 1 (I) collagen [Col1A1]: Forward 5′-CCCGGGTTTCAGAGACA ACTTC-3′, Reverse 5′-TCCACATGCTTTATTCCAGCAATC-3′; TGF-β1: Forward 5′-AGCGACTCGCCAGAGTGGTTA-3′, Reverse 5′-GCAGTG TGTTATCCCTGCTGTCA-3′; SP1: Forward 5′-TCGGATGAGCTACA GAGGCACAA-3′, Reverse 5′-GTCACTCCTCATGAAGCGCTTAGG-3′; and GAPDH: Forward 5′-GCACCGTCAAGGCTGAGAAC-3′, Reverse 5′-TGGTGAAGACGCCAGTGGA-3′) with an Applied Biosystems Prism 7500 (Applied Biosystems, Foster City, CA, USA). To detect miRNA expression, the RT reaction was performed using the TaqMan MicroRNA Assay (Applied Biosystems) according to the manufacturer's instructions. The GAPDH level was measured and used to normalize the relative abundance of mRNAs and miRNAs.

Immunoblot. Proteins (20–50 μg) were subjected to sodium dodecyl sulfate–polyacrylamide gel electrophoresis and then transferred onto Immobilon P membranes. After blocking, the membranes were treated with primary antibodies, followed by peroxidase-conjugated secondary antibodies. Immunoreactive bands were visualized by the enhanced chemiluminescence system using the Fujifilm Image Reader LAS-3000 (Fuji Medical Systems, Stamford, CT, USA).

Transient transfection of miRNA precursors. Precursors of miR-29b, -143, and -218, and the negative control were transfected into human stellate cells using Lipofectamine 2000 (Invitrogen, Carlsbad, CA, USA) at a final concentration of 50 nM. Briefly, the cells were plated in DMEM supplemented with 10% FBS at a density of 1–2 × 10^5 cells/ml 24 h prior to the transfection. miRNA precursors and Lipofectamine 2000 were mixed at a ratio of 25 (pmol):1 (μl) in Opti-MEM I Reduced Medium (Invitrogen) and incubated for 20–30 min at room temperature. The miRNA precursor–Lipofectamine 2000 complexes were then added to stellate cell culture medium. After 6 h, the culture medium was changed, and TGF-β1 was added at a concentration of 2 ng/ml.

Luciferase reporter assay. 3′UTRs containing putative miRNA target regions of the Col1A1 and SP1 genes were obtained by PCR using human stellate cell cDNA as a template and primer sets as follows: Col1A1–miR-29: Forward 5′-TTCTCGAGGTTCTTGTCTTG ATGTGTCACC-3′, Reverse 5′-TTTCTAGAGAGAGCAGAGGCCTGAGA AG-3′; Col1A1–miR-143: Forward 5′-CTCGAGACTCCCTCCATCCCAA CCT-3′, Reverse 5′-TCTAGAATTGCTGGGCAGACAATAC-3′; Col1A1–miR-218: Forward 5′-CTCGAGGTGGATGGGGACTTGTGAAT-3′, Reverse 5′-TCTAGATTATGTTTGGGTCATTTCCAC-3′; SP1–miR-29: Forward 5′-TTCTCGAGTGGGTGCTACACAGAATGC-3′, Reverse 5′-TTTC TAGAAGACTGTCCTTATTTCCTTGGTA-3′; and SP1–miR-218: Forward 5′-CTCGAGGATGTTTTCCCTTAACTTTTCCT-3′, Reverse 5′-TCT AGACTAAAAGCTTATATCCTCAGCATC-3′. Each of the forward and reverse primers carried the *Xho*I and *Xba*I sites at their 5′-ends. The obtained DNA fragments were inserted into the pmirGLO Vector (Promega, San Luis Obispo, CA, USA). The resulting vectors were dubbed pCol1A1–miR-29/mirGLO, pCol1A1–miR-143/mirGLO, pCol1A1–miR-218/mirGLO, pSP1–miR-29/mirGLO, and pSP1–miR-218/mirGLO. Human stellate cells were seeded on 96-well plates (Microtest 96-well Assay Plate; Becton Dickinson, Franklin Lakes, NJ, USA) in DMEM supplemented with 10% FBS at a density of 2 × 10^4 cells/well. The following day, they were transfected with 200 ng of reporter plasmid along with miRNA precursors using Lipofectamine 2000 as described above and incubated for an additional 24 h. After incubation, the medium was removed from the wells, and 20 μl of phosphate-buffered saline was added. The Dual-Glo Luciferase Assay System (Promega) was used to analyze luciferase expression according to the manufacturer's protocol. Firefly luciferase activity was normalized to *Renilla* luciferase activity to adjust for variations in transfection efficiency among experiments.

Statistical analysis. Data presented as bar graphs are the means ± SD of at least three independent experiments. Statistical analysis was performed using Student's *t*-test, and $P < 0.05$ was considered significant.

Results and discussion

Regulation of Col1A1 expression by TGF-β1 and IFNα in human stellate cells

Immortalized human stellate cells, LX-2, are classified as an activated phenotype that expresses mRNAs for Col1A1 and other fibrogenetic molecules and are reported to be highly gene-transfectable [24]. At first, we observed that Col1A1 mRNA expression increased dose-dependently by TGF-β1 (Fig. 1A), whereas this upregulation was significantly inhibited by the presence of 100 IU/ml of human IFNα (Fig. 1B).

Extraction of miR-29b, -143, and -218 as candidates interacting with Col1A1 3′UTR

To determine the role of miRNAs in human stellate cell collagen expression, we searched for predictable miRNAs that could interact

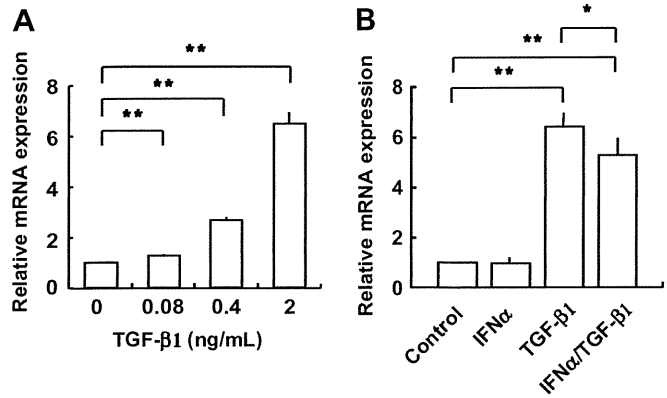

Fig. 1. Regulation of alpha 1 (I) collagen (Col1A1) expression in human stellate cells. (A) Dose-dependent effect of TGF-β1 on Col1A1 mRNA expression. Human stellate cells, LX-2, were treated with TGF-β1 (0, 0.08, 0.4, and 2 ng/ml) for 24 h in DMEM containing 0.1% FBS. (B) Effect of IFNα on Col1A1 mRNA expression in human stellate cells stimulated with TGF-β1. The cells were treated with IFNα (100 IU/ml), TGF-β1 (2 ng/ml), or IFNα (100 IU/ml) + TGF-β1 (2 ng/ml) for 24 h in DMEM containing 0.1% FBS. Control: human stellate cells were cultured for 24 h in DMEM containing 0.1% FBS. mRNA expression was analyzed by real-time PCR. The results are expressed as relative expression against control expression without treatment. $^{*}P < 0.05$; $^{**}P < 0.01$.

with 3′UTR of human Col1A1 mRNA using TargetScan Human Release 5.1 (http://www.targetscan.org/). As a result, miR-29, -98, -129, -133, -143, -196, -218, and let-7 were extracted as candidates. Because further *in silico* analyses among the eight candidates indicated that miR-29b, -143, and -218 were highly homologous to the Col1A1 3′UTR, we checked the expression levels of these miRNAs in human stellate cells by real-time PCR. As a result, miR-143 and -218 expressions were up and downregulated dose-dependently by TGF-β1, respectively, (Fig. 2A and B). Although miR-29b expression was unaffected by TGF-β1, it increased in

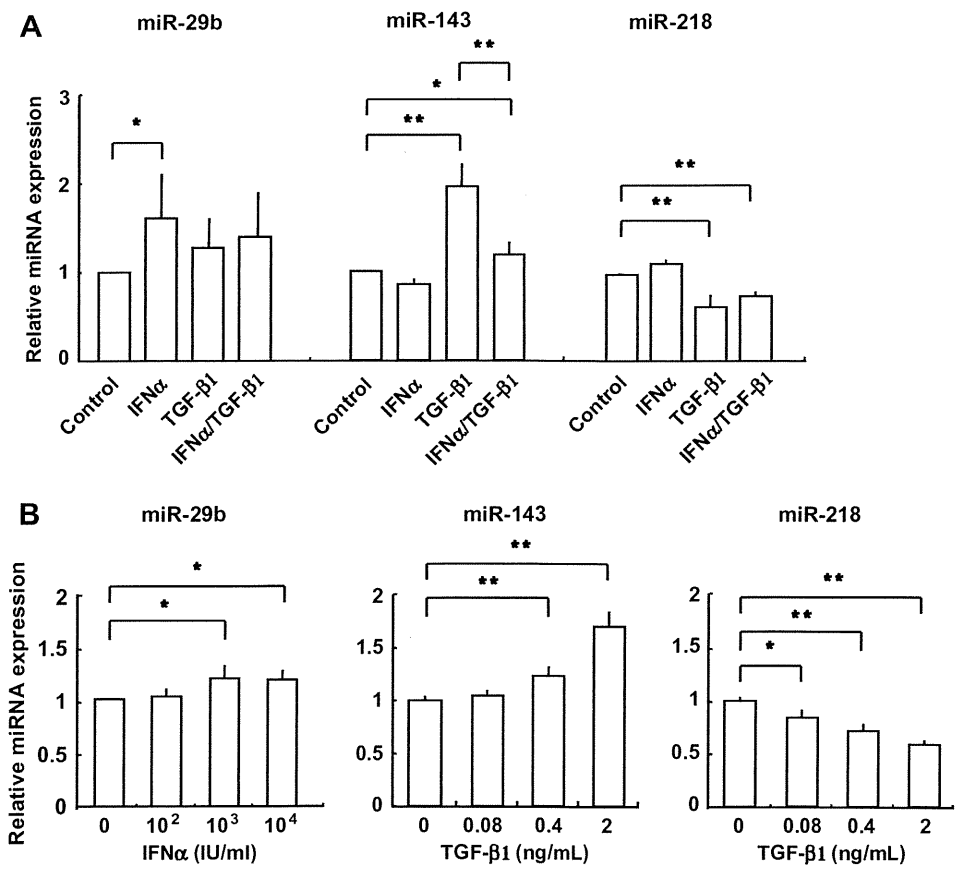

Fig. 2. Expression of miR-29b, -143, and -218 in human stellate cells. (A) Expression of miR-29b, -143, and -218 in human stellate cells, LX-2. The cells were treated with IFNα (100 IU/ml), TGF-β1 (2 ng/ml), or IFNα (100 IU/ml) + TGF-β1 (2 ng/ml) for 24 h in DMEM containing 0.1% FBS. Control: human stellate cells were cultured for 24 h in DMEM containing 0.1% FBS. (B) Dose-dependent effect of IFNα or TGF-β1 on the expression of miR-29b, -143, and -218 in human stellate cells. miRNA expression was analyzed by real-time PCR. The results are expressed as relative expression against control expression without treatment. $^{*}P < 0.05$; $^{**}P < 0.01$.

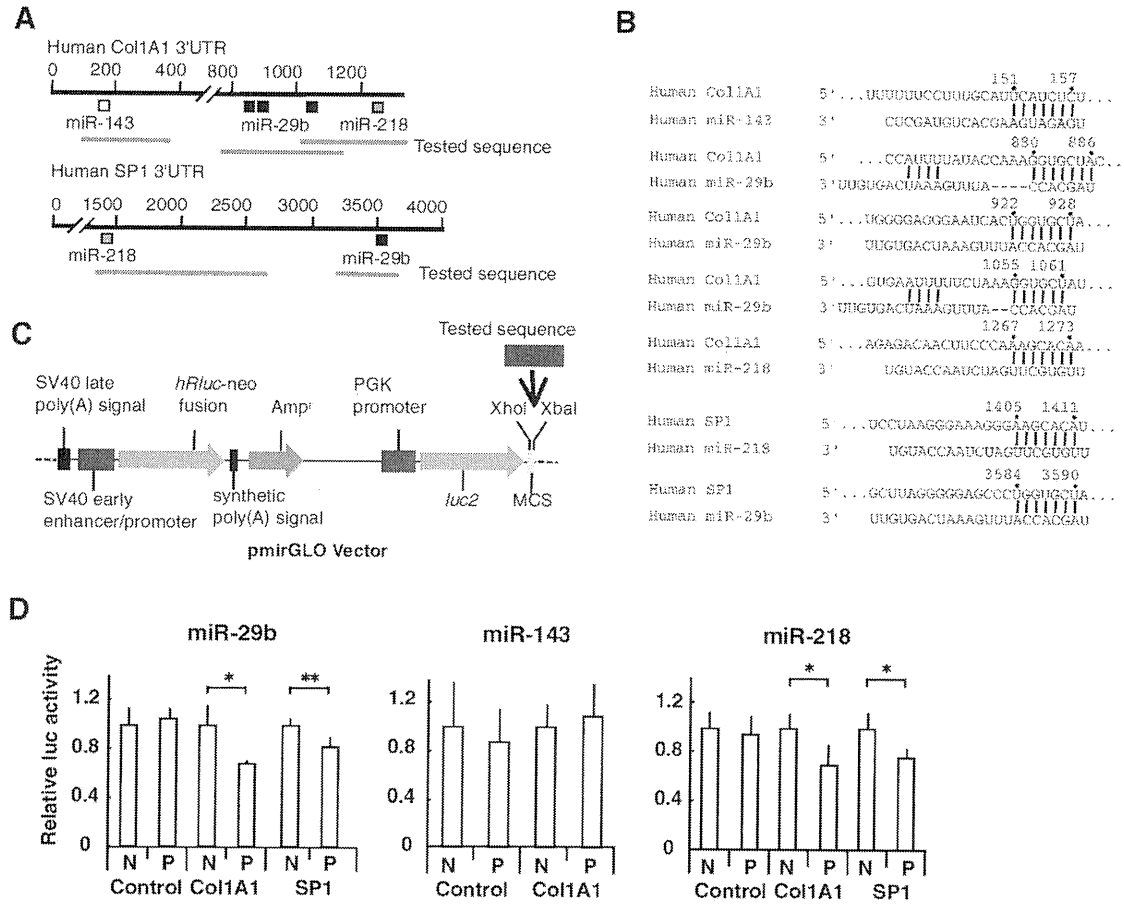

Fig. 3. Interaction of miR-29b, -143, and -218 with the 3′UTRs of alpha 1 (I) collagen (Col1A1) and SP1 mRNAs. (A) Schematic indication of the miRNA binding sites in the 3′UTRs of Col1A1 and SP1 mRNAs based on TargetScan Human Release 5.1 (http://www.targetscan.org/). Each black, white, and gray box indicates miR-29b, -143, and -218, respectively. Tested sequences indicate the regions that were inserted into the luciferase reporter vector. (B) Predicted consequential pairing of the target region and miRNAs. Arabic numerals above indicate the positions relative to the 3′UTR start sites. (C) Luciferase reporter vector structure. The vector contained two expression units; one for the *Renilla* luciferase gene (*hRluc*-neo fusion) expression. This unit was driven by an SV40 early promoter. The other was for the firefly luciferase gene (*luc2*). This unit was driven by a human phosphoglycerate kinase (PGK) promoter and contained multiple cloning sites (MCS) downstream of the *luc2* sequence. Each Col1A1 and SP1 3′UTR containing a putative miRNA target region (tested sequence) was cloned into the MCS. Arrows indicate the gene directions. Amp^R indicates an ampicillin-resistant plasmid gene. (D) Interaction of miR-29b, -143, and -218 with the 3′UTRs of Col1A1 and SP1 mRNAs in human stellate cells. Relative luciferase activity derived from pCol1A1–miR-29/mirGLO and pSP1–miR-29/mirGLO in the presence of miR-29b precursors (left panel), pCol1A1–miR-143/mirGLO in the presence of miR-143 precursors (center panel), and pCol1A1–miR-218/mirGLO and pSP1–miR-218/mirGLO in the presence of miR-218 precursors (right panel). The pmirGLO vector was used as a negative control reporter vector (control). N: cotransfection of reporter vectors along with negative control precursors, which have a scrambled sequence. P: cotransfection of reporter vectors along with miRNA precursors. Firefly and *Renilla* luciferase activities were determined, and firefly luciferase was normalized to *Renilla* luciferase activity. Results are expressed as relative activities against the activity in the presence of negative control precursors. $^{*}P < 0.05$ and $^{**}P < 0.01$.

the presence of IFNα (Fig. 2A and B). Thus, we assumed that these miRNAs might affect type I collagen expression via their interaction with Col1A1 3′UTR in human stellate cells.

Interaction of miR-29b, -143, and -218 with 3′UTRs of Col1A1 and SP1 mRNAs

The prediction of miRNA target regions on Col1A1 3′UTR by TargetScan indicated that Col1A1 3′UTR has three target regions for miR-29b, one for miR-143, and one for miR-218 (Fig. 3A and B). Because collagen gene expression is regulated by miR-192 via an interaction with the transcriptional repressor E-box [26], we additionally considered SP1, which is a transcriptional regulator of Col1A1 expression induced by TGF-β1 [27,28]. The predicted miRNA target regions of SP1 3′UTR contained one target region for miR-29b and one for miR-218 (Fig. 3A and B).

To investigate the direct targeting of Col1A1 by miR-29b, -143, and -218 and that of SP1 by miR-29b and -218, the sequence of each target region was cloned and inserted into the downstream region of the firefly luciferase reporter gene (Fig. 3C). The resulting vectors were dubbed pCol1A1–miR-29/mirGLO, pCol1A1–miR-143/mirGLO, pCol1A1–miR-218/mirGLO, pSP1–miR-29/mirGLO, and pSP1–miR-218/mirGLO. These vectors were cotransfected into human stellate cells with miRNA precursors. As a result, the miR-29b and -218 precursors inhibited luciferase activity derived from the vectors carrying Col1A1 or SP1 3′UTRs (Fig. 3D). In contrast, the miR-143 precursors had no effect on luciferase activity of the vector carrying Col1A1 3′UTR (Fig. 3D). According to these observations, we assumed that the Col1A1 and SP1 3′UTR sequences could be targeted by miR-29b and -218, whereas miR-143, which was induced by TGF-β1 (Fig. 2A and B), had a negligible effect on Col1A1 expression in human stellate cells.

Regulation of type I collagen expression by miR-29b and -218

Next, we examined the effect of miR-29b and -218 overexpression on type I collagen mRNA and protein expression in human stellate cells. Transient transfection of miR-29b precursors signifi-

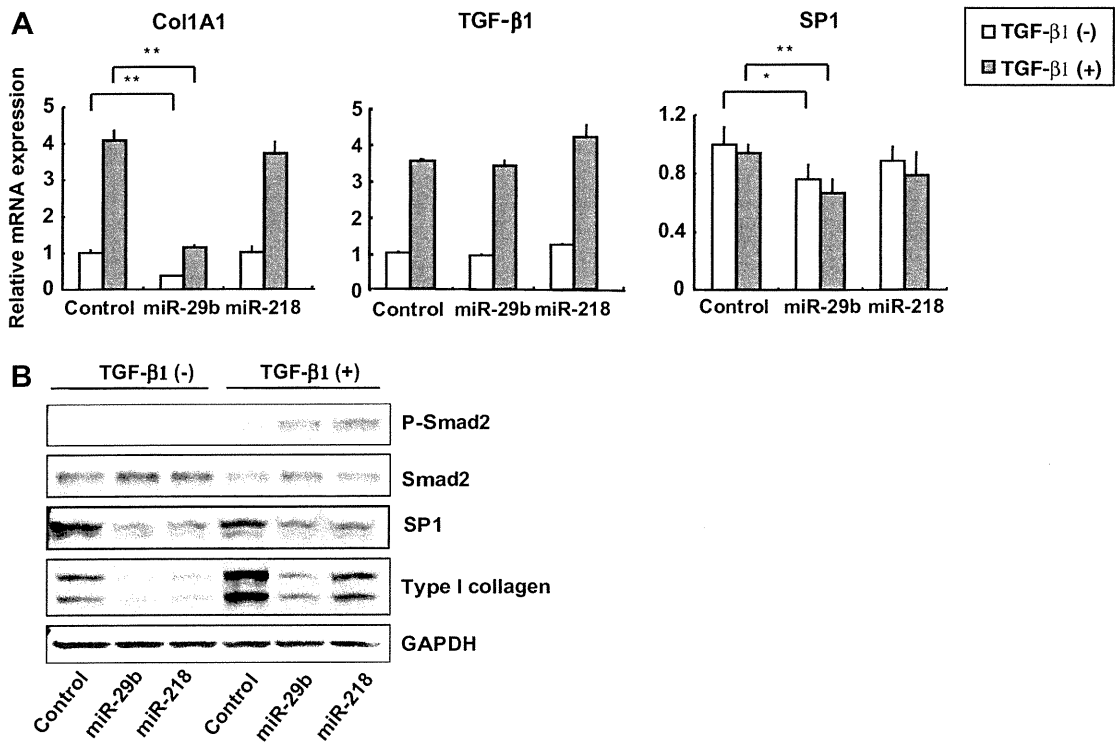

Fig. 4. Effect of miR-29b and -218 on type I collagen expression in human stellate cells. Human stellate cells were cultured in DMEM supplemented with 10% FBS and were transfected with 50 nM miR-29b, -218 precursors, or a negative control, which had a scrambled sequence (control) using Lipofectamine 2000. After 6 h, the medium was changed to DMEM containing 0.1% FBS with or without 2 ng/ml TGF-β1, and the culture was continued for another 24 h. (A) Effect of miR-29b and -218 precursors on the expression of Col1A1, TGF-β1, and SP1 mRNAs in human stellate cells with (gray column) or without (white column) TGF-β1. mRNA expression was analyzed by real-time PCR. The results are expressed as relative expression against control expression. $^{*}P < 0.05$; $^{**}P < 0.01$. (B) Effect of miR-29b and -218 precursors on the protein expression of phospho-Smad2 (P-Smad2), Smad2, SP1, type I collagen, and GAPDH in human stellate cells in the presence (+) or absence (−) of TGF-β1.

cantly inhibited type I collagen mRNA and protein expression (Fig. 4A, left panel, and B) in unstimulated human stellate cells. Additionally, transfection of miR-29b precursors completely suppressed the upregulation of type I collagen mRNA and protein under TGF-β1 stimulation. TGF-β1 stimulation induces Col1A1 mRNA expression through a pathway that includes SP1 and phosphorylated Smad2/3 [29]. In our results, upregulation of TGF-β1 mRNA (Fig. 4A, center panel) and phosphorylation of Smad2 (Fig. 4B) under TGF-β1 stimulation were unaffected by the transfection of miR-29b precursors. These results suggested that miR-29b may affect the downstream of phosphorylated Smad2. Moreover, the transfection of miR-29b precursors decreased SP1 mRNA and protein expression (Fig. 4A, right panel, and B). Thus, the miR-29b-induced repression of type I collagen expression could be caused by its direct interaction with Col1A1 3′UTR and additionally by its interaction with SP1 expression in human stellate cells. These observations agree with a report showing the role of miR-29 in collagen expression and cardiac fibrosis after cardiac infarction [30]. In contrast, transfection of miR-218 precursors triggered a negligible change in Col1A1 and SP1 mRNA expression (Fig. 4A, left and right panels) but slightly reduced their protein level (Fig. 4B). Taken together, these results imply that miR-29b is the most potent miRNA with regard to collagen production in human stellate cells.

Conclusions

We found a potent repression of collagen production by miR-29b in human stellate cells. IFNs attenuate and may regress liver fibrosis caused by hepatitis C viral infection [21–23], although the precise molecular mechanism has yet to be demonstrated. The present study using human stellate cells demonstrated that IFNα upregulates miR-29b (Fig. 2B and C), which is a negative regulator of type I collagen production via the interaction with Col1A1 and SP1 3′UTRs. This observation implies the contribution of miR-29b to antifibrotic IFN actions. Targeted delivery of miR-29b to activated stellate cells in the liver could become a new therapeutic strategy for human liver fibrosis in the future.

Acknowledgment

This work was supported by a grant from the Ministry of Health, Labour and Welfare of Japan to N. Kawada (2008–2009).

References

[1] R. Bataller, D.A. Brenner, Hepatic stellate cells as a target for the treatment of liver fibrosis, Semin. Liver Dis. 21 (2001) 437–451.
[2] S.L. Friedman, Molecular regulation of hepatic fibrosis, an integrated cellular response to tissue injury, J. Biol. Chem. 275 (2000) 2247–2250.
[3] N. Kawada, The hepatic perisinusoidal stellate cell, Histol. Histopathol. 12 (1997) 1069–1080.
[4] S. Dooley, B. Delvoux, B. Lahme, K. Mangasser-Stephan, A.M. Gressner, Modulation of transforming growth factor beta response and signaling during transdifferentiation of rat hepatic stellate cells to myofibroblasts, Hepatology 31 (2000) 1094–1106.
[5] E. Albanis, S.L. Friedman, Hepatic fibrosis. Pathogenesis and principles of therapy, Clin. Liver Dis. 5 (2001) 315–334. v–vi.
[6] W. Filipowicz, S.N. Bhattacharyya, N. Sonenberg, Mechanisms of post-transcriptional regulation by microRNAs: are the answers in sight?, Nat Rev. Genet. 9 (2008) 102–114.
[7] D.P. Bartel, MicroRNAs: genomics, biogenesis, mechanism, and function, Cell 116 (2004) 281–297.
[8] J. Brennecke, D.R. Hipfner, A. Stark, R.B. Russell, S.M. Cohen, Bantam encodes a developmentally regulated microRNA that controls cell proliferation and regulates the proapoptotic gene hid in *Drosophila*, Cell 113 (2003) 25–36.

[9] G.M. Schratt, F. Tuebing, E.A. Nigh, C.G. Kane, M.E. Sabatini, M. Kiebler, M.E. Greenberg, A brain-specific microRNA regulates dendritic spine development, Nature 439 (2006) 283–289.
[10] C.Z. Chen, L. Li, H.F. Lodish, D.P. Bartel, MicroRNAs modulate hematopoietic lineage differentiation, Science 303 (2004) 83–86.
[11] J. Kota, R.R. Chivukula, K.A. O'Donnell, E.A. Wentzel, C.L. Montgomery, H.W. Hwang, T.C. Chang, P. Vivekanandan, M. Torbenson, K.R. Clark, J.R. Mendell, J.T. Mendell, Therapeutic microRNA delivery suppresses tumorigenesis in a murine liver cancer model, Cell 137 (2009) 1005–1017.
[12] J.F. Chen, E.P. Murchison, R. Tang, T.E. Callis, M. Tatsuguchi, Z. Deng, M. Rojas, S.M. Hammond, M.D. Schneider, C.H. Selzman, G. Meissner, C. Patterson, G.J. Hannon, D.Z. Wang, Targeted deletion of Dicer in the heart leads to dilated cardiomyopathy and heart failure, Proc. Natl. Acad. Sci. USA 105 (2008) 2111–2116.
[13] D.O. Perkins, C.D. Jeffries, L.F. Jarskog, J.M. Thomson, K. Woods, M.A. Newman, J.S. Parker, J. Jin, S.M. Hammond, MicroRNA expression in the prefrontal cortex of individuals with schizophrenia and schizoaffective disorder, Genome Biol. 8 (2007) R27.
[14] I.M. Pedersen, G. Cheng, S. Wieland, S. Volinia, C.M. Croce, F.V. Chisari, M. David, Interferon modulation of cellular microRNAs as an antiviral mechanism, Nature 449 (2007) 919–922.
[15] J. Ji, J. Shi, A. Budhu, Z. Yu, M. Forgues, S. Roessler, S. Ambs, Y. Chen, P.S. Meltzer, C.M. Croce, L.X. Qin, K. Man, C.M. Lo, J. Lee, I.O. Ng, J. Fan, Z.Y. Tang, H.C. Sun, X.W. Wang, MicroRNA expression, survival, and response to interferon in liver cancer, N. Engl. J. Med. 361 (2009) 1437–1447.
[16] C.E. Rogler, L. Levoci, T. Ader, A. Massimi, T. Tchaikovskaya, R. Norel, L.E. Rogler, MicroRNA-23b cluster microRNAs regulate transforming growth factor-beta/bone morphogenetic protein signaling and liver stem cell differentiation by targeting Smads, Hepatology 50 (2009) 575–584.
[17] C. Esau, S. Davis, S.F. Murray, X.X. Yu, S.K. Pandey, M. Pear, L. Watts, S.L. Booten, M. Graham, R. McKay, A. Subramaniam, S. Propp, B.A. Lollo, S. Freier, C.F. Bennett, S. Bhanot, B.P. Monia, MiR-122 regulation of lipid metabolism revealed by in vivo antisense targeting, Cell Metab. 3 (2006) 87–98.
[18] L. Zheng, G.C. Lv, J. Sheng, Y.D. Yang, Effect of miRNA-10b in regulating cellular steatosis level by targeting PPAR-alpha expression, a novel mechanism for the pathogenesis of NAFLD, J. Gastroenterol. Hepatol. (2009).
[19] J. Ji, J. Zhang, G. Huang, J. Qian, X. Wang, S. Mei, Over-expressed microRNA-27a and 27b influence fat accumulation and cell proliferation during rat hepatic stellate cell activation, FEBS Lett. 583 (2009) 759–766.
[20] C.J. Guo, Q. Pan, D.G. Li, H. Sun, B.W. Liu, MiR-15b and miR-16 are implicated in activation of the rat hepatic stellate cell: an essential role for apoptosis, J. Hepatol. 50 (2009) 766–778.
[21] Y. Shiratori, F. Imazeki, M. Moriyama, M. Yano, Y. Arakawa, O. Yokosuka, T. Kuroki, S. Nishiguchi, M. Sata, G. Yamada, S. Fujiyama, H. Yoshida, M. Omata, Histologic improvement of fibrosis in patients with hepatitis C who have sustained response to interferon therapy, Ann. Intern. Med. 132 (2000) 517–524.
[22] T. Poynard, J. McHutchison, G.L. Davis, R. Esteban-Mur, Z. Goodman, P. Bedossa, J. Albrecht, Impact of interferon alfa-2b and ribavirin on progression of liver fibrosis in patients with chronic hepatitis C, Hepatology 32 (2000) 1131–1137.
[23] Y. Inagaki, T. Nemoto, M. Kushida, Y. Sheng, K. Higashi, K. Ikeda, N. Kawada, F. Shirasaki, K. Takehara, K. Sugiyama, M. Fujii, H. Yamauchi, A. Nakao, B. De Crombrugghe, T. Watanabe, I. Okazaki, Interferon alfa down-regulates collagen gene transcription and suppresses experimental hepatic fibrosis in mice, Hepatology 38 (2003) 890–899.
[24] L. Xu, A.Y. Hui, E. Albanis, M.J. Arthur, S.M. O'Byrne, W.S. Blaner, P. Mukherjee, S.L. Friedman, F.J. Eng, Human hepatic stellate cell lines, LX-1 and LX-2: new tools for analysis of hepatic fibrosis, Gut 54 (2005) 142–151.
[25] K. Otogawa, T. Ogawa, R. Shiga, K. Nakatani, K. Ikeda, Y. Nakajima, N. Kawada, Attenuation of acute and chronic liver injury in rats by iron-deficient diet, Am. J. Physiol. Regul. Integr. Comp. Physiol. 294 (2008) R311–R320.
[26] M. Kato, J. Zhang, M. Wang, L. Lanting, H. Yuan, J.J. Rossi, R. Natarajan, MicroRNA-192 in diabetic kidney glomeruli and its function in TGF-beta-induced collagen expression via inhibition of E-box repressors, Proc. Natl. Acad. Sci. USA 104 (2007) 3432–3437.
[27] L. Li, C.M. Artlett, S.A. Jimenez, D.J. Hall, J. Varga, Positive regulation of human alpha 1 (I) collagen promoter activity by transcription factor Sp1, Gene 164 (1995) 229–234.
[28] I. Garcia-Ruiz, P. de la Torre, T. Diaz, E. Esteban, I. Fernandez, T. Munoz-Yague, J.A. Solis-Herruzo, Sp1 and Sp3 transcription factors mediate malondialdehyde-induced collagen alpha 1 (I) gene expression in cultured hepatic stellate cells, J. Biol. Chem. 277 (2002) 30551–30558.
[29] P. Sysa, J.J. Potter, X. Liu, E. Mezey, Transforming growth factor-beta1 up-regulation of human alpha(1) (I) collagen is mediated by Sp1 and Smad2 transacting factors, DNA Cell Biol. 28 (2009) 425–434.
[30] E. van Rooij, L.B. Sutherland, J.E. Thatcher, J.M. DiMaio, R.H. Naseem, W.S. Marshall, J.A. Hill, E.N. Olson, Dysregulation of microRNAs after myocardial infarction reveals a role of miR-29 in cardiac fibrosis, Proc. Natl. Acad. Sci. USA 105 (2008) 13027–13032.

Cell Transplantation, Vol. 18, pp. 665–675, 2009

0963-6897/09 $90.00 + .00
E-ISSN 1555-3892
www.cognizantcommunication.com

Hepatocytes From Fibrotic Liver Possess High Growth Potential in Vivo

Manabu Nishie,*† Chise Tateno,*[1] Rie Utoh,*[2] Toshihiko Kohashi,‡
Norio Masumoto,*‡ Naoya Kobayashi,† Toshiyuki Itamoto,‡ Noriaki Tanaka,†
Toshimasa Asahara,‡ and Katsutoshi Yoshizato*§[1]

*Yoshizato Project, CLUSTER, Hiroshima Prefectural Institute of Industrial Science and Technology, Hiroshima 739-0046, Japan
†Department of Surgery, Okayama University Graduate School of Medicine and Dentistry, Okayama 700-8558, Japan
‡Department of Surgery, Division of Frontier Medical Science, Program for Biomedical Research, and Hiroshima University 21st Century COE Program for Advanced Radiation Casualty Medicine, Graduate School of Biomedical Sciences, Hiroshima University, Hiroshima 734-8551, Japan
§Developmental Biology Laboratory and Hiroshima University 21st Century COE Program for Advanced Radiation Casualty Medicine, Department of Biological Science, Graduate School of Science, Hiroshima University, Hiroshima 739-8526, Japan

Hepatocyte transplantation is effective for treating liver failure, but healthy donors as a source of hepatocytes are quite limited. The livers of patients with hepatic fibrosis could be an alternative source; however, few reports have examined the nature of hepatocytes from fibrotic livers (f-hepatocytes). In this study, we compared the growth of f-hepatocytes and hepatocytes from normal livers (n-hepatocytes). Hepatocytes were isolated from normal and CCl_4-treated wild-type Fischer rats that express dipeptidyl dipeptidase IV (DPPIV) gene ($DPPIV^+$). The n- and f-hepatocytes proliferated in culture at similar rates. Both types of hepatocytes were transplanted into $DPPIV^-$ mutant Fischer rats that had been treated with retrorsine to injure the liver and were partially hepatectomized (PHx) before transplantation. Both n- and f-$DPPIV^+$-hepatocytes proliferated and formed colonies. The colony sizes of f-hepatocytes 21 days posttransplantation were approximately three times those of n-hepatocytes. The hepatocytes were analyzed using a fluorescence activated cell sorter (FACS). The FACS profile differed between f- and n-hepatocytes: f-hepatocytes were less granular, less autofluorescent, and smaller than n-hepatocytes. These characteristics of f-hepatocytes resembled those reported for small-sized n-hepatocytes (SHs), which are highly proliferative and preferentially express a unique set of 10 SH genes. However, f-hepatocytes preferentially expressed only five of the SH genes. The expression profile of f-hepatocytes was rather similar to that of proliferating n-hepatocytes in the regenerating liver after PHx. The f-hepatocytes were morphologically normal and did not show any preneoplastic phenotype. These normal and proliferative natures of f-hepatocytes in vivo suggest the fibrotic liver as a source of hepatocytes for transplantation.

Key words: Hepatocyte transplantation; Liver regeneration; Hepatocyte proliferation; Hepatectomy; Retrorsine; Carbon tetrachloride

INTRODUCTION

The liver cell transplantation therapy for a damaged liver was first reported in 1993, in which hepatocytes ($1–60 \times 10^7$ cells) were autotransplanted into the spleen of cirrhosis or chronic hepatitis patients (11). The donor cells lived for up to 11 months. Strom et al. transplanted less than 1.2×10^9 allogeneic hepatocytes into the spleen as a bridge to the ensuing liver transplantation (14). The patients who received hepatocyte transplantation before liver transplantation had an average survival of 3.8 ± 3.3 days versus 2.8 ± 2.5 days for those without hepatocyte transplantation. Although the survival period did not differ statistically, hepatocyte transplantation improved serum ammonia, cerebral blood flow, and intracranial pressure. Two of 30 patients were able to recover with hepatocyte transplantation alone without usual liver transplantation (14).

Patients with metabolic diseases have been also subjected to hepatocyte transplantation in some cases. For

Received October 31, 2008; final acceptance March 30, 2009.
[1]Present address: PhoenixBio Co., Ltd., PhoenixBio. Co. Ltd., 3-4-1 Kagamiyama, Higashishiroshima, Hiroshima 739-0046, Japan.
[2]Present address: Tokyo Women's Medical University, Institute of Advanced Biomedical Engineering and Science, Kawada-cho 8-1, Shinjuku-ku, Tokyo 162-8666, Japan.
Address correspondence to Katsutoshi Yoshizato, Ph.D., PhoenixBio. Co. Ltd., 3-4-1 Kagamiyama, Higashishiroshima, Hiroshima, 739-0046, Japan. Tel: 81-82-431-0016; Fax: 81-82-431-0017; E-mail: katsutoshi.yoshizato@phoenixbio.co.jp

example, an ornithine transcarbamoylase (OTC)-deficient 5-year-old patient was transplanted with 1.7×10^9 normal hepatocytes. The patient improved symptomatically but died from pneumonia 43 days posttransplantation (15). When a 10-year-old patient with Crigler-Najjar syndrome was transplanted with 7.5×10^9 hepatocytes, an amount approximately equal to 5% of the entire liver, the patient was able to decrease the serum bilirubin to a half the level before liver transplantation (4). Recently, a patient with glycogen storage disease type Ib caused by a deficiency of glucose-6-phosphate transporter was treated with hepatocyte transplantation, which resulted in normalization of glucose-6-phosphatase activity in the liver, and substantial improvement in quality of life (9).

These previous studies show that the transplantation of hepatocytes equivalent to 1–5% of the total hepatocytes in the liver is therapeutically effective. Cell transplantation is easier, safer, and less expensive than liver transplantation, and can be performed repeatedly. The major challenge to hepatocyte transplantation is the shortage of transplantable cells owing to the limited availability of healthy donors (16). Hepatocytes from fibrotic livers (f-hepatocytes) are a potential source of hepatocytes for transplantation because of their greater availability over hepatocytes from normal livers (n-hepatocytes). Mito et al. isolated n- and f-hepatocytes from rats and transplanted each of them into the syngenic rat spleen (10). Although the yield and viability of the f-hepatocytes were lower than the n-hepatocytes, and their features were different from the normal counterpart in some aspects, they were able to continue to proliferate for 6 months after transplantation. However, the proliferative ability of f-hepatocytes has not been characterized in the liver, which is of prime importance when they are utilized as the cells for transplantation.

This study aimed to characterize the growth of f-hepatocytes using rats as a model animal. The adult rat liver contains a minor population of hepatocytes called small hepatocytes (SHs) (6,17,19). These cells are smaller and have greater replicative potential than typical parenchymal hepatocytes (PHs). SHs have been characterized using an "SH fraction" that contaminated PHs. Previously, we isolated a PH-free SH fraction and SH-free PH fraction from the adult rat liver using a fluorescence-activated cell sorter (FACS) combined with centrifugal elutriation and characterized the hepatocytes in the fraction. These hepatocytes were designated as pure SHs or R3Hs and pure large hepatocytes (LH) or R2Hs in our previous study, respectively (2). For the sake of simplicity, we call pure SHs 'SHs" and pure LHs "LHs" in this study and assume that "hepatocytes" consist of LHs and SHs. SHs were mononuclear and of lower ploidy. Previously, we identified 10 genes that are preferentially expressed in SHs: *p55cdc, hydroxysteroid sulfotransferase (Sta), cytochrome P450 17 (CYP17), prostaglandin E2 receptor EP3 subtype (Pge2r), pancreatic secretory trypsin inhibitor (Psti), Cdc2, connexin 26 (Cx26), mitotic centromere-associated kinesin (Mcak), rat EST 207254*, and an unknown gene (*ab088476*) (2). These genes are referred to as the SH-associated genes.

We isolated n- and f-hepatocytes from rats. The f-hepatocytes were characterized in terms of size, FACS profile, in vitro and in vivo proliferation ability, and gene expression, and were compared with n-hepatocytes and hepatocytes in the regenerating liver (r-hepatocytes). As a result, we clearly demonstrated that f-hepatocytes are different from LHs, are similar to SHs in proliferation ability, and are similar to r-hepatocytes in their gene expression profile.

MATERIALS AND METHODS

Treatment of Animals

Dipeptidyl dipeptidase IV-deficient ($DPPIV^-$) mutant male Fischer rats aged 9–10 weeks were purchased from Charles River Japan, Inc. (Yokohama, Japan) and their wild-type ($DPPIV^+$) counterparts from Japan SLC, Inc. (Shizuoka, Japan). Liver fibrosis was induced by intramuscular injection of $DPPIV^+$ rats with CCl_4 at 1 ml/kg body weight, twice a week, for 6 weeks. Hepatocytes were isolated from the rats 6 weeks postinjection. $DPPIV^+$ male Fischer rats aged 15–16 weeks were subjected to two thirds partial hepatectomy (PHx). Then, r-hepatocytes were isolated from the rats 36 h after PHx.

Hepatocyte Isolation

$DPPIV^+$ male Fischer rats aged 15–16 weeks were divided into three groups, one used for normal controls, second for CCl_4 treatment, and the last for PHx experiment. The n-, f-, and r-hepatocytes were isolated from these rats using the two-step collagenase perfusion method (6), and were collected by centrifugation at $50 \times g$ for 2 min. The pellets were centrifuged through 45% Percoll at $50 \times g$ for 24 min (6). These pellets were centrifuged again at $50 \times g$ for 2 min, and the final pellets were used as hepatocytes, which consisted of LHs and SHs. In our previous study, PHs and SHs were obtained as the pellet and supernatant, respectively, after centrifugation of the original hepatocyte preparations at $50 \times g$ for 1 min (17). The hepatocyte preparation used in the present study corresponds to this previous preparation consisting of PHs and SHs. The viability of the hepatocytes was determined by Trypan blue exclusion. The n-, f-, and r-hepatocytes were subjected to FACS analysis, and to determining the cell diameter (17) and the gene expression levels. In addition, the proliferation ability of n- and f-hepatocytes was assayed in vitro and in vivo.

FACS Analysis

Hepatocytes were analyzed using a cell sorter (FACS Vantage; Becton Dickinson, Mountain View, CA) with a 100-μm nozzle, as reported previously (17). Fluorescence excited at 488 nm was measured through 530-nm (FL1) and 575-nm (FL2) filters with 4-decade logarithmic amplification. To measure the physical characteristics of the cells, linear amplification was used for the forward scatter, which is a measure of cell size, and 4-decade logarithmic amplification was used for the side scatter (SCC), which is a measure of cytoplasmic complexity. The optical bench was calibrated at a fixed amplitude and photomultiplier voltage using fluorescent polystyrene beads (Fluorosbrite Calibration Grade 6-μm YG microspheres; Polysciences, Warrington, PA), and the instrument was used in the conditions under which these beads fell in the same peak channels. Propidium iodide was added to the cell suspensions to be analyzed, at a concentration of 1 μg/ml. The cells that excluded the dye were analyzed as viable cells. Data obtained from the FACS experiments were analyzed using Cell Quest software (Becton Dickinson).

Determination of the Growth Potential of Hepatocytes In Vitro

The n- and f-hepatocytes were cocultured with mitomycin C-treated Swiss 3T3 cells on Celldesks in HCGM culture medium (i.e., Dulbecco's modified Eagle's medium supplemented with 10% fetal bovine serum, 20 mM *N*-2-hydroxyethylpiperazine-*N'*-2-ethane sulfonic acid, 30 μg/ml L-proline, 0.5 μg/ml insulin, 10^{-7} M dexamethasone, 44 mM $NaHCO_3$, 10 mM nicotinamide, 10 ng/ml EGF, 0.2 mM L-ascorbic acid 2-phosphate, 100 IU/ml penicillin G, and 100 μg/ml streptomycin) (1,13, 17–19). They were incubated in a 5% CO_2/95% air atmosphere at 37°C. Swiss 3T3 cells were seeded on the hepatocytes 24 h after the hepatocytes were plated. The growth potential of the hepatocytes was determined at 10 days, as previously shown (17).

Hepatocyte Transplantation

DPPIV$^-$ rats weighing 130–140 g were given two intraperitoneal injections of retrorsine at 30 mg/kg body weight, 2 weeks apart. Four weeks after the last injection, a two thirds PHx was performed (6,8). The n- and f-hepatocytes (1.5×10^5) isolated from the DPPIV$^-$ rats were transplanted into the retrorsine-treated partial hepatectomized (retrorsine/PHx) DPPIV$^-$ rats via the portal vein. Some rats were killed 48 h after transplantation to measure the engraftment rate of the transplanted hepatocytes, the ratio of transplanted cells to cells integrated to the liver plate. Other rats were killed 21 days after transplantation. Tissues from each lobe of the liver were frozen until use for enzyme-histochemical or immunohistochemical analyses.

Enzyme-Histochemical and Immunohistochemical Staining

DPPIV enzyme histochemistry was performed on 10-μm-thick cryosections that had been prepared from the liver, fixed in ice-cold acetone for 5 min, air-dried, and washed for 5 min in ice-cold 95% ethanol. The sections were air-dried and incubated for 40–60 min in a substrate reagent consisting of 0.5 mg/ml Gly-Pro-methoxy-β-naphthylamide (Sigma Chemical, St. Louis, MO), 1 mg/ml Fast Blue BB (Sigma Chemical), 100 mmol/L Tris-maleate (pH 6.5), and 100 mmol/L NaCl. Then, the sections were washed with PBS and fixed in 10% formaldehyde. All tissue sections were counterstained with hematoxylin.

Cryosections were fixed in –20°C acetone for 5 min and subjected to immunohistochemistry to detect liver-related proteins. The primary antibodies (Abs) used were as follows: anti-rat DPPIV mouse monoclonal antibody (gift from Dr. D. C. Hixson, Rhode Island Hospital), anti-rat albumin rabbit antiserum (a hepatocyte marker; Cappel, Durham, NC), anti-human α-smooth muscle actin (SMA) mouse monoclonal antibody (an activated stellate cell marker; MBL, Nagoya, Japan), anti-rat glutathione-*S*-transferase (a preneoplastic hepatocyte marker, GST-P) rabbit antiserum (MBL), OV6 mouse monoclonal antibody (an oval cell marker; gift from Dr. D.C. Hixson) (5), and anti-human cytokeratin 19 monoclonal antibody (CK19; a bile duct cell and oval cell marker; Amersham). The primary Abs were visualized with Alexa 488-labeled goat anti-mouse-IgG or Alexa 594-labeled goat anti-rabbit IgG (Molecular Probes, Eugene, OR).

Morphometric Analysis

Livers were isolated from rats 48 h after transplantation, weighed, and processed for cryosectioning and DPPIV staining. The approximate numbers of hepatocytes per gram of liver were calculated from the liver weight using the value $115 \times 10^6 \pm 15 \times 10^6$ hepatocytes/g liver (12). DPPIV$^+$ and DPPIV$^-$ hepatocytes were counted in arbitrary areas visualized on tissue sections, and the numerical ratio of the former to the latter was calculated as the occupancy rate of engrafted hepatocytes in the liver. The number of engrafted hepatocytes per liver was calculated by multiplying the occupancy rate of the engrafted hepatocytes by the total number of host hepatocytes per liver. The engraftment index (the numerical ratio of engrafted hepatocytes to injected hepatocytes on transplantation) was calculated by dividing the number of engrafted hepatocytes per liver by the number of injected hepatocytes.

A transplanted hepatocyte homes to the liver, starts to replicate there, and forms a colony soon after transplantation. The area of colonies formed by the transplanted hepatocytes was measured using NIH image var. 1.62, and the data were analyzed using StatView ver. 5.0 (SAS Institute, Cary, NC). The colony size increases as engrafted hepatocytes proliferate. The volume of a colony was estimated using a reported method (6). Briefly, we made 10-μm-thick semiserial sections from liver specimens, at 100-μm intervals. Different parts of a DPPIV$^+$ colony were seen in several different serial sections when the diameter of the colony exceeded 100 μm, which is a colony area corresponding to >7,850 μm^2. We selected the section in which the longest diameter of a particular DPPIV$^+$ colony was seen and calculated the colony area using this diameter. For a colony with a diameter <100 μm, we assumed that the diameter measured in a section was the longest diameter and calculated the colony area using this diameter. We only measured the colonies consisting of more than eight DPPIV$^+$ transplanted hepatocytes. The colonies were oval or round. To quantify the area of these colonies, 40 portal areas were examined in each animal at 21 days posttransplantation. The volume of a colony was calculated from the area of the colony, assuming that the colony was spherical and that the cross section was made along the maximum diameter of the sphere. To calculate the mean diameter of cells in colonies formed by the transplanted hepatocytes, the area and cell number therein were measured for 10 colonies. The mean cell number in a colony was calculated using the area or volume of the colony and the mean cell diameter of hepatocytes.

Quantification of mRNA

Total RNA was purified from n-, f-, and r-hepatocytes using an RNeasy minikit (QIAGEN K.K., Tokyo, Japan) and was treated with an RNase-free DNase set (QIAGEN). cDNA was synthesized using PowerScript reverse transcriptase (Clontech, Palo Alto, CA) and was amplified with a set of gene-specific primers (2) and SYBR Green PCR mix in a PRISM 7700 Sequence Detector (Applied Biosystems, Tokyo, Japan). A series of diluted plasmid cDNAs containing each gene was used to plot the standard amplification curves. The mRNA copy numbers in cDNA samples were calculated using the standard amplification curves (2).

Statistical Analysis

The area of colonies formed by the transplanted hepatocytes was measured using NIH image ver. 1.62, and the data were analyzed using StatView ver. 5.0 (SAS Institute, Cary, NC). The significance of differences was analyzed using the Mann-Whitney rank sum test. A value of $p < 0.05$ was considered significant.

RESULTS

Size and FACS Characterization of Hepatocytes

We prepared n- and f-hepatocytes from normal and CCl_4-treated rats, respectively. The yield of the n- and f-hepatocytes was $35.0 \pm 19.0 \times 10^6$ and $2.6 \pm 1.5 \times 10^6$ cells per animal ($n = 3$), respectively, and their viability was $95.5 \pm 0.6\%$ and $69.6 \pm 2.2\%$ ($n = 3$), respectively. Similarly, r-hepatocytes were isolated from rats 36 h after PHx. These cells were placed on nonadhesive dishes to determine their diameters as a measure of cell size. The n-, f-, and r-hepatocytes had diameters of 22.1 ± 0.2, 20.1 ± 0.2, and 21.5 ± 1.0 μm, respectively. Previously, we had found diameters of 23.2 ± 0.5 and 17.4 ± 0.0 μm for LHs and SHs, respectively (2).

The shape of contour lines in FACS analysis were variable from experiment to experiment, depending on the axis adjustment of the cell souter that is usually made and fixed in each series of experiment. We always compared the level of FL1 (autoflorescence) and SSC (granularity) of experimental cells (f- and r-hepatocytes in this study) with control cells (n-hepatocytes). It was confirmed that the similar differences of f-hepatocytes over n-hepatocytes and that of r-hepatocytes over n-hepatocytes were reproducibly observed in three independent analyses. The FACS analysis showed that f-hepatocytes were totally different from n-hepatocytes (Fig. 1A). Most of the f-hepatocytes were less granular and less autofluorescent. The FACS profile of r-hepatocytes was similar to that of n-hepatocytes, although the former contained more populations with low granularity and low autofluorescence than the latter (Fig. 1B).

Growth Ability of n- and f-Hepatocytes

The n- and f-hepatocytes were isolated from three normal rats and four CCl_4-treated rats, respectively, and then cultured with Swiss 3T3 cells in HCGM for 10 days. The ratios of the cell number at day 10 to that at day 1 were 3.5 ± 1.0 and 3.3 ± 0.1 for f- and n-hepatocytes ($n = 3$), respectively, clearly indicating similar growth ability between the two types of hepatocytes in vitro.

The growth ability in vivo was compared between n- and f-hepatocytes. DPPIV$^+$ n- and f-hepatocytes were transplanted into DPPIV$^-$ retrorsine/PHx rats via the portal vein. The livers were harvested 48 h after transplantation. The DPPIV$^+$ n- and f-hepatocytes were counted on the host liver sections. The engraftment index of f-hepatocytes obtained by two transplantation experiments was 12.3% and 7.4% (average 9.9%), which was similar to that of n-hepatocytes, 13.0% and 5.6% (9.3%). A previous study revealed that oval cells were not seen

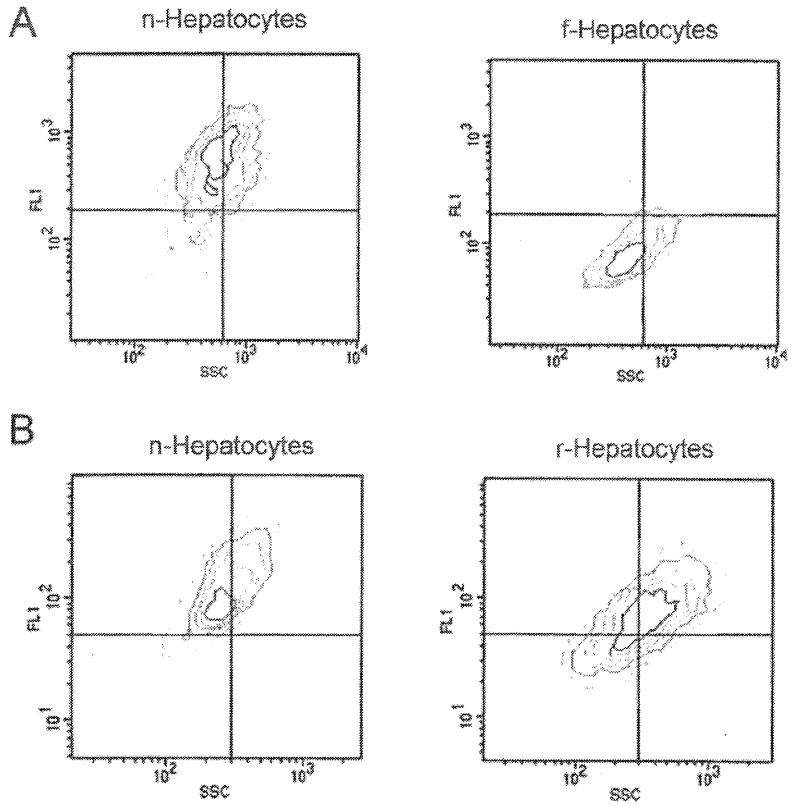

Figure 1. FACS profiles of hepatocytes. Two series (A, B) of experiments were performed in which hepatocytes were analyzed by FACS in terms of the side scatter (SSC) and fluorescence through 530-nm filter (FL1). (A) One series compared the FACS profiles of n- and f-hepatocytes, and (B) the other compared the profiles of n- and r-hepatocytes.

in the livers of CCl_4-treated rats (3). In the present study, serial liver sections were immunostained for DPPIV and an oval cell marker, OV6. There were no DPPIV and OV6 double-positive cells (data not shown), showing the absence of oval cells in the hepatocyte preparations used in this study.

Retrorsine/PHx DPPIV$^-$ rats were transplanted with n- and f-hepatocytes that had been isolated from four DPPIV$^+$ rats each as described above, killed 21 days after transplantation, and their livers were processed for DPPIV$^+$ enzyme histochemistry (Fig. 2). The f-hepatocyte colonies were more heterogeneous in size and appeared larger than the n-hepatocyte colonies, suggesting higher growth potential of the former than the latter. To quantitatively evaluate the growth ability, we measured two parameters on histological sections, the colony area and volume. Area size distribution of the hepatocyte colonies was determined and is shown in Figure 3, which confirmed the above suggestions of higher size heterogeneity and larger colony area of f-hepatocytes than those of n-hepatocytes. The mean colony area was calculated from these graphs and is shown in Table 1. f-Hepatocytes formed colonies whose areas were approximately 2.4-fold larger (significant at $p < 0.05$) than those of n-hepatocytes. The diameter of the hypothetical sphere formed by the transplanted hepatocytes was measured and also is shown in Table 1. As expected, the colony volume of f-hepatocytes was approximately 3.7-fold larger (significant at $p < 0.05$) than that of n-hepatocytes. From the mean area and volume of colonies formed by the transplanted hepatocytes, we estimated the replication potential of a transplanted cell. To simplify the calculation, we assumed that transplanted hepatocytes were spherical, and we calculated the number of transplanted cells per area and volume of a colony as described in the Materials and Methods. As shown in Table 2, the number of transplanted cells per area and volume of a colony was about 1.9- and 2.6-fold larger than that of n-hepatocytes, respectively. The average numbers of cell divisions for transplanted f- and n-hepatocytes over 21 days were calculated to be 11–13 and 9–11, respectively (Table 2). From these measurements, we concluded that f-hepatocytes have higher growth potential than n-hepatocytes in vivo.

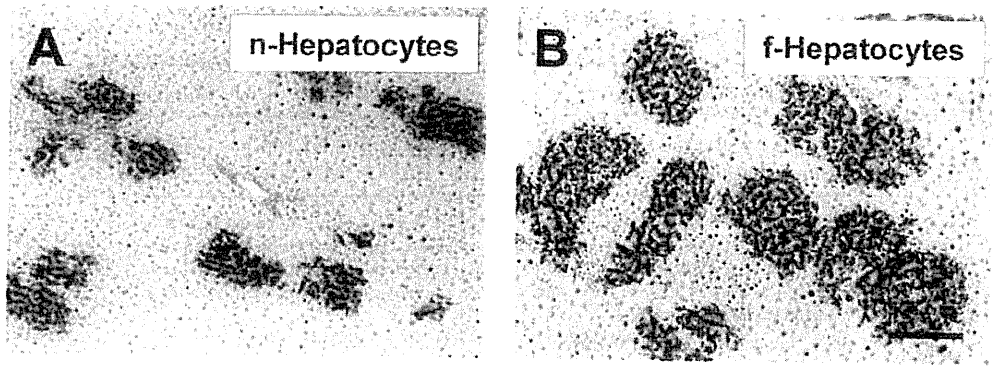

Figure 2. Colonies formed by transplanted hepatocytes. (A) DPPIV$^+$ n-hepatocytes and (B) DPPIV$^+$ f-hepatocytes were transplanted into the livers of retrorsine/PH DPPIV$^-$ rats. Liver sections were prepared from the rats 21 days after transplantation. Cryosections of the livers were subjected to DPPIV histochemical staining. The transplanted hepatocytes were stained black. Scale bar: 200 μm.

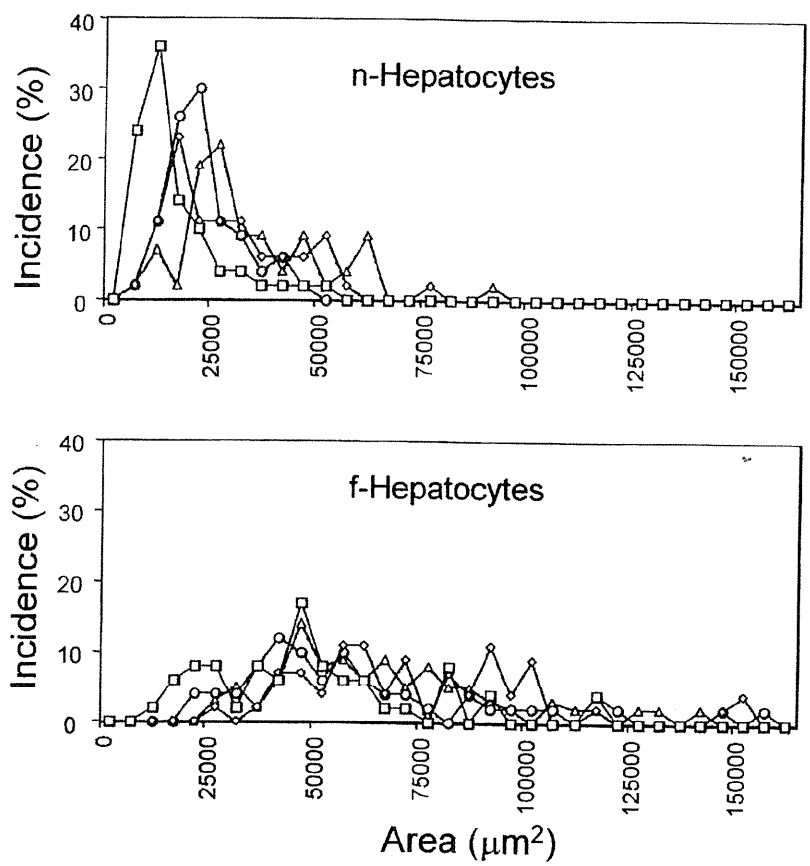

Figure 3. Size distribution of the hepatocyte colonies. Forty regions were selected randomly from DPPIV-stained sections for four individuals as shown in Figure 2 and were photographed. The colony area was measured on the photographs using NIH ver. 1.62. Each line represents the proportion (%) of the area measured for each of the four animals. f-Hepatocytes occupied more area than n-hepatocytes.

Table 1. The Mean Area and Volume of Colonies Formed by Transplanted Hepatocytes

Transplanted Cells	Area (μm^2)	Volume (μm^3)	Number
n-Hepatocytes	26,387 ± 1,015 *	3,580,888 ± 212,285 *	211
f-Hepatocytes	64,450 ± 2,016 *	13,207,708 ± 628,909 *	206

Hepatocytes were transplanted into the livers of rats, which were killed 21 days after transplantation. The areas of colonies were measured for four different rats transplanted with hepatocytes under the identical experimental conditions, as shown in Figure 2. The mean ± SE of areas and volumes of colonies was calculated from these measurements.
*$p < 0.05$. The p-values were determined by Mann-Whitney rank sum test.

Cell Phenotype in Colonies Formed by Transplanted Hepatocytes

The cells in the colonies of n- and f-hepatocytes were characterized in terms of the expression of four lineage-specific markers of liver cells: albumin, α-SMA, CK19, and GST-P. The cells in colonies of both types of hepatocytes expressed albumin at a high level, comparable to that of the surrounding host hepatocytes (Fig. 4A–D). Neither CK19 nor GST-P was expressed in the cells of colonies formed by both types of hepatocytes (data not shown), supporting the notion that f-hepatocytes do not show preneoplastic or bile duct epithelial cell phenotypes. These results strongly suggest that f-hepatocytes retain the phenotype of normal hepatocytes and maintain the normal phenotype throughout replication. In addition, α-SMA$^+$ cells (activated stellate cells) were not observed in the f-hepatocyte-transplanted livers (Fig. 4G, H) as in the n-hepatocyte-transplanted livers (Fig. 4E, F).

Gene Expression in f-Hepatocytes

Previously, we had identified 10 SH-associated genes: *p55cdc, Sta, CYP17, Pge2r, Psti, Cdc2, Cx26, Mcak, rat EST 207254*, and an unknown gene (*ab088476*) (2). The mRNA expression levels of all of these genes except *rat EST 207254* were determined using real-time RT-PCR in n-, f-, and r-hepatocytes (Fig. 5B, Table 3) and were compared with our previous data, which are shown in Figure 5A. The expression levels of the SH-associated genes were much higher in SHs than in LHs (Fig. 5A). The expression levels of four genes (*ab088476, Pge2r, Cx26*, and *Psti*) were similar between n- and f-hepatocytes. By contrast, five genes (*CYP17, p55cdc, Cdc2, Mcak*, and *Sta*) were expressed at much higher levels in f-hepatocytes than in n-hepatocytes. It was noteworthy that the overall expression profile of n-hepatocytes was similar to that of r-hepatocytes (Fig. 5B).

DISCUSSION

Fibrotic livers have been characterized mainly with respect to activated stellate cells, which are known as extracellular matrix (ECM)-producing cells, and little is known about the nature of hepatocytes in the fibrotic liver. Mito et al. reported that hepatocytes from fibrotic liver exhibited greater proliferation than hepatocytes from normal liver when transplanted into the spleen, despite the injection of approximately 1/200 of the amount of normal cells (10). Histological observations revealed that transplanted hepatocytes from cirrhotic livers differentiated into plates two to several cells thick, whereas plates of one-cell thickness prevailed with the transplantation of normal hepatocytes. One interpretation of this observation is that cirrhotic hepatocytes are still in the regenerating phase. Hepatocytes from cirrhotic livers retained normal functions such as glycogenesis and albumin synthesis (10). On electron micrographs, collagen fibers in the space of Disse were observed 1 year after the transplantation of hepatocytes from cirrhotic livers, but were not present with normal hepatocyte transplantation (10). In the present study, we characterized hepatocytes isolated from the fibrotic liver for the first time in

Table 2. Mean Cell Number in a Colony

Transplanted Cells	Cell Diameter (μm)	Cell Number per Colony Area	Cell Number per Colony Volume	Cell Divisions During 21 Days
n-Hepatocytes	22.8 ± 0.5	110 ± 12	1,217 ± 206	9–11
f-Hepatocytes	20.3 ± 0.3	209 ± 21	3,131 ± 481	11–13

Data are expressed as the mean ± SE.

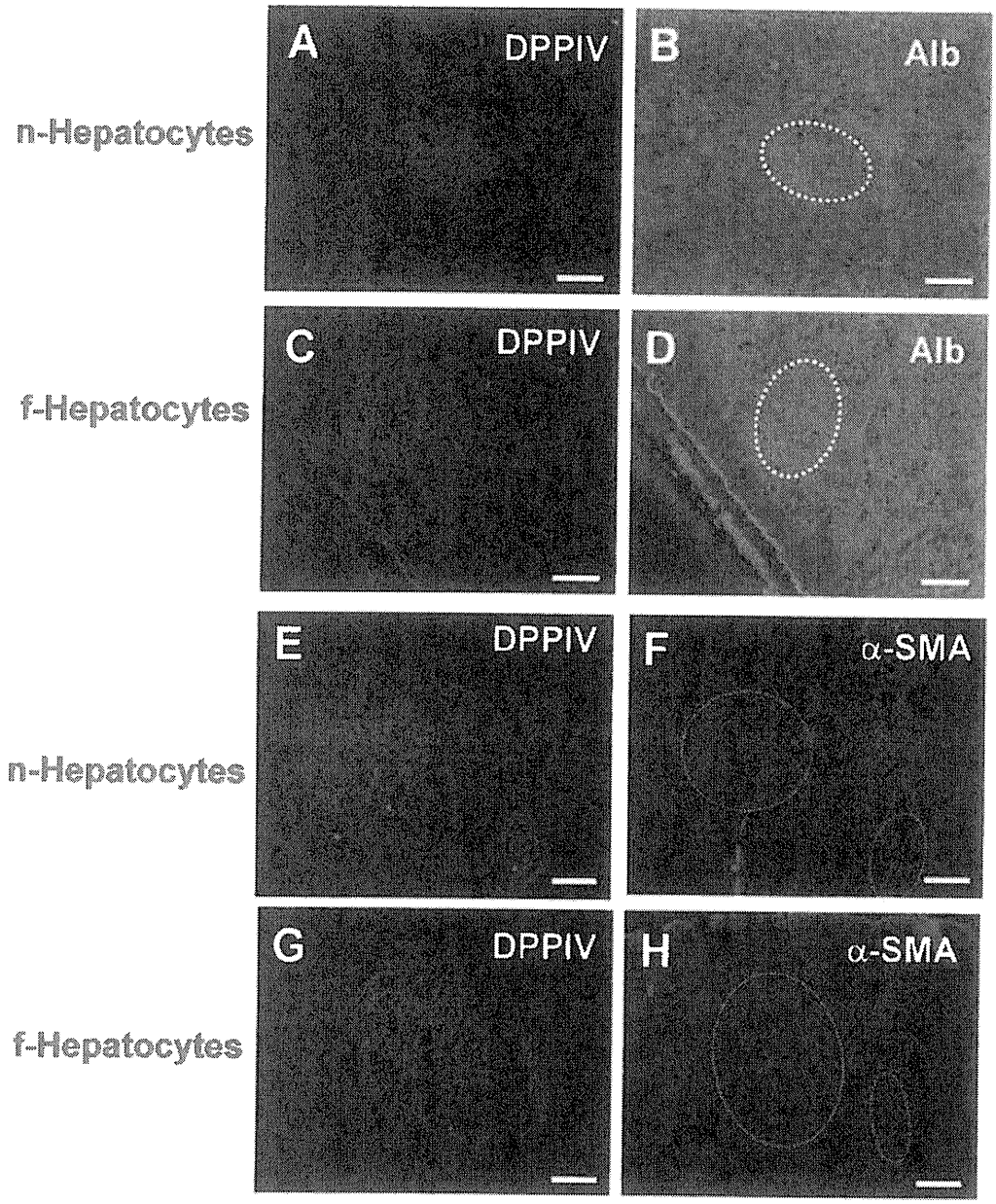

Figure 4. Phenotypes of the cells in the colonies formed by transplanted hepatocytes. DPPIV$^+$ n-hepatocytes (A, B, E, and F) and DPPIV$^+$ f-hepatocytes (C, D, G, and H) were transplanted into retrorsine/PH-treated DPPIV$^-$ rats. Serial liver cryosections were prepared 21 days after transplantation and were stained for DPPIV (A, C, E, and G), albumin (B and D), and α-SMA (F and H). The colonies formed by the transplanted hepatocytes are localized as DPPIV$^+$ regions (A, C, E, and G). These colonies are each marked by broken lines on the corresponding immunostained serial sections (B, D, F, and H). The DPPIV$^+$ cells were all albumin$^+$. There were no α-SMA$^+$ cells in the livers transplanted with both n- and f-hepatocytes. Scale bar: 100 μm.

terms of their growth potential in vitro and in vivo (in the retrorsine/PH rat liver), FACS profile, cell size, growth potential, and gene expression.

The growth potential of hepatocytes is heterogeneous: the hepatocyte with the greatest proliferative ability forms a colony consisting of more than 100 cells within 10 days, whereas the hepatocyte with the lowest ability does not divide (19). The adult rat liver contains a minor population of hepatocytes called SHs, which have a smaller size and higher replicative potential than LHs (6,17,19). Previously, we had used FACS and centrifugal elutriation to isolate highly proliferative SHs as

cells with low autofluorescence and low granularity (2). In the present study, most of the f-hepatocytes had low autofluorescence and low granularity, similar to SHs. Therefore, we investigated whether f-hepatocytes have characteristics similar to SHs in terms of size, growth potential in vitro and in vivo, and gene expression.

The average diameter of f-hepatocytes (20.1 ± 0.2 μm) was comparable to that of n-hepatocytes (22.1 ± 0.2

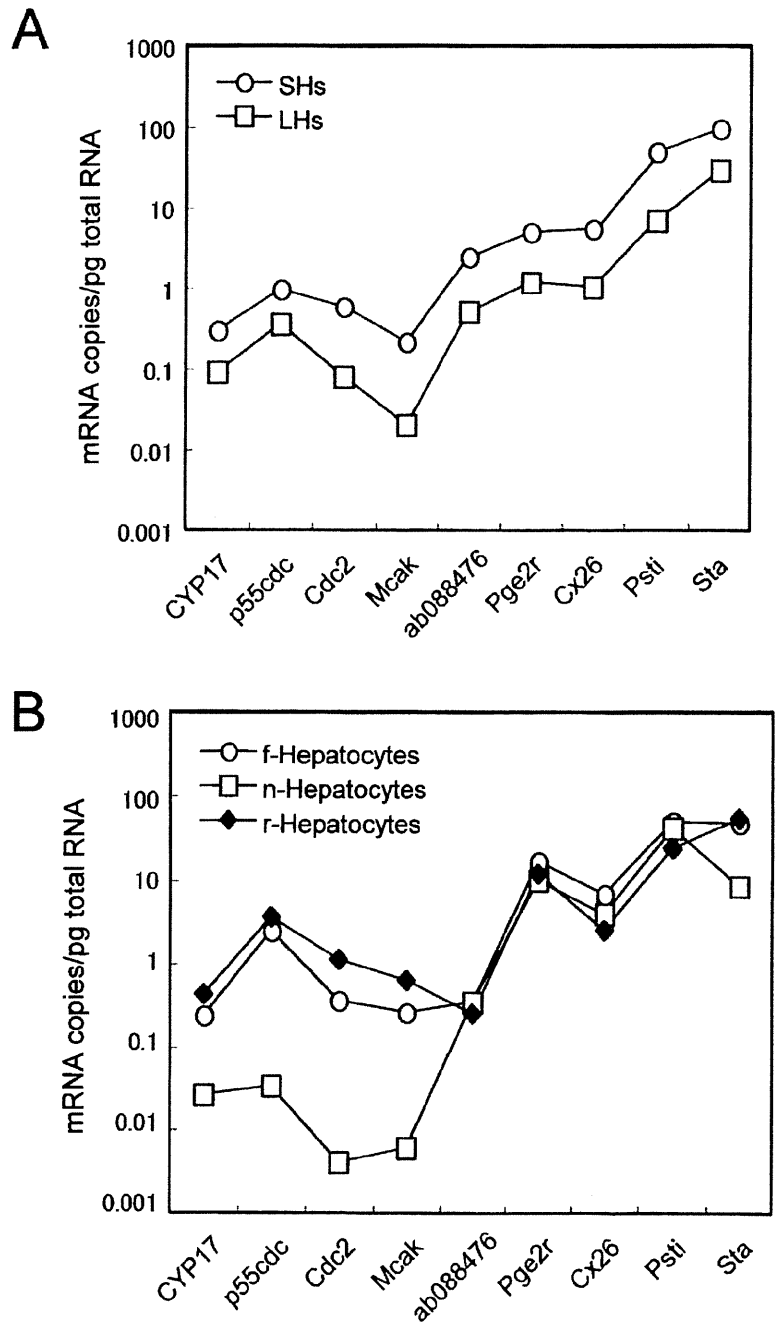

Figure 5. Expression of the SH-associated genes in hepatocytes. (A) Gene expression levels in SHs and LHs. This graph is drawn using the mRNA expression data presented in Tables 4 and 5 of Asahina et al. (2). (B) The gene expression levels in n-, f-, and r-hepatocytes were determined by measuring the mRNA copy number using real-time RT-PCR.

Table 3. Expression Levels of SH-Associated Genes in n-, r-, and f-Hepatocytes

Gene*	mRNA Copies/pg Total RNA		
	n-Hepatocytes	f-Hepatocytes	r-Hepatocytes
CYP17	0.026 ± 0.000	0.239 ± 0.147	0.430 ± 0.216
p55cdc	0.032 ± 0.022	2.443 ± 3.138	3.527 ± 1.044
Cdc2	0.004 ± 0.004	0.360 ± 0.424	1.092 ± 0.397
Mcak	0.006 ± 0.008	0.259 ± 0.308	0.627 ± 0.197
Unknown (*ab088476*)	0.343 ± 0.566	0.339 ± 0.281	0.252 ± 0.032
Pge2r	9.770 ± 8.698	16.452 ± 11.455	11.557 ± 1.699
Cx26	3.870 ± 0.967	6.690 ± 2.426	2.481 ± 0.267
Psti	40.961 ± 9.499	48.189 ± 11.954	23.374 ± 9.560
Sta	8.429 ± 7.905	46.431 ± 36.094	52.897 ± 21.741

The primers used for real-time RT-PCR have been reported elsewhere (2). Each value represents the mean ± SD of three different rats.
*Genes identified as differentially expressed using a cDNA microarray and representational difference analysis in SHs (2).

μm) but was larger than that of SHs (17.4 ± 0.0 μm). The growth of f-hepatocytes in vitro was compared with that of n-hepatocytes. Previously, we had shown that SH proliferation was about four times that of LHs in vitro (17). The f-hepatocytes showed growth ability similar to that of n-hepatocytes. SHs were also highly proliferative in vivo (about three times compared with LHs), as determined by colony-forming ability after transplantation into the livers of the retrorsine/PH rats (6). Here, we also estimated the growth potential of hepatocytes using this model. The engraftment index obtained in this study at 48 h after transplantation was 9.9% for f-hepatocytes and 9.3% for n-hepatocytes, and did not differ significantly. The colonies formed by transplanted cells at 21 days were examined in all of the residual livers of the recipients and showed that f-hepatocytes were more proliferative (about 2.5 times) than n-hepatocytes.

From the data, we concluded that f-hepatocytes have higher growth ability than n-hepatocytes in vivo but not in vitro. At present, there is no explanation for this apparent discrepancy between the in vivo and in vitro growth abilities of the two types of hepatocytes. However, it seems that the culture conditions used in the present study were not sufficient for f-hepatocytes to exhibit their full proliferation potential.

Ten SH-associated genes had been identified previously (2). We examined whether f-hepatocytes also express the SH-associated genes, and we compared the expression of SH-associated genes between f- and r-hepatocytes. The f-hepatocytes expressed five of the nine SH genes, at similar levels as SHs. Importantly, the overall expression profile of f-hepatocytes resembled that of r-hepatocytes.

The expression of marker proteins specific to hepatocytes, preneoplastic hepatocytes, and bile duct epithelial cells was characterized in f-hepatocytes. When rats were treated with CCl_4 for more than 7 weeks, morphologically recognizable GST-P$^+$ preneoplastic nodules were observed in some of the treated rats (7). In the present study, the cells in colonies formed by transplanted f-hepatocytes were albumin$^+$ but CK19$^-$ and GST-P$^-$, like n-hepatocytes, showing that the cells in the f-hepatocyte colonies expressed hepatocyte markers but not bile duct or preneoplastic markers. In addition, stellate cells did not express α-SMA in the f-hepatocyte colonies. There seems to be a regulatory mechanism in vivo under which f-hepatocytes stably express hepatocytic phenotypes but do not express biliary phenotypes.

In this study, we demonstrated that hepatocytes surrounded by ECM in the fibrotic liver retained high growth potential. f-Hepatocytes can be used instead of n-hepatocytes for hepatocyte transplantation, although the yield of hepatocytes from a fibrotic liver is fewer than that from a normal liver. However, it remains to be determined whether human f-hepatocytes have similar normal and proliferative phenotypes as rat f-hepatocytes, when isolated from the livers of fibrotic patients and transplanted into normal recipients. If they show these phenotypes, fibrotic livers could be a useful source of hepatocytes for the treatment of liver damage using hepatocyte transplantation.

ACKNOWLEDGMENTS: We thank Mss. Y. Yoshizane, H. Kohno, Y. Matsumoto, and S. Nagai for technical assistance, and Drs. M. Mito and K. Asahina for valuable advice. This work was supported by a grant from the Cooperative Link of Unique Science and Technology for Economy Revitalization (CLUSTER), Japan.

REFERENCES

1. Asahina, K.; Sato, H.; Yamasaki, C.; Kataoka, M.; Shiokawa, M.; Kataoka, S.; Tateno, C.; Yoshizato, K. Pleio-

trophin/heparin-binding growth-associated molecule as a mitogen of rat hepatocytes and its role in regeneration and development of liver. Am. J. Pathol. 160:2191–2205; 2002.
2. Asahina, K.; Shiokawa, M.; Ueki, T.; Yamasaki, C.; Aratani, A.; Tateno, C.; Yoshizato, K. Multiplicative mononuclear small hepatocytes in adult rat liver: Their isolation as a homogeneous population and localization to periportal zone. Biochem. Biophys. Res. Commun. 342: 1160–1167; 2006.
3. Dabeva, M. D.; Alpini, G.; Hurston, E.; Shafritz, D. A. Models for hepatic progenitor cell activation. Proc. Soc. Exp. Biol. Med. 204:242–252; 1993.
4. Fox, I. J.; Chowdhury, J. R.; Kaufman, S. S.; Goertzen, T. C.; Chowdhury, N. R.; Warkentin, P. I.; Dorko, K.; Sauter, B. V.; Strom, S. C. Treatment of the Crigler-Najjar syndrome type I with hepatocyte transplantation. N. Engl. J. Med. 338:1422–1426; 1998.
5. Hixson, D. C.; Chapman, L.; McBride, A.; Faris, R.; Yang, L. Antigenic phenotypes common to rat oval cells, primary hepatocellular carcinomas and developing bile ducts. Carcinogenesis 18:1169–1175; 1997.
6. Katayama, S.; Tateno, C.; Asahara, T.; Yoshizato, K. Size-dependent in vivo growth potential of adult rat hepatocytes. Am. J. Pathol. 158:97–105; 2001.
7. Kohashi, T.; Tateaki, Y.; Tateno, C.; Asahara, T.; Obara, M.; Yoshizato, K. Expression of pleiotrophin in hepatic nonparenchymal cells and preneoplastic nodules in carbon tetrachloride-induced fibrotic rat liver. Growth Factors 20: 53–60; 2002.
8. Laconi, E.; Oren, R.; Mukhopadhyay, D. K.; Hurston, E.; Laconi, S.; Pani, P.; Dabeva, M. D.; Shafritz, D. A. Long-term, near-total liver replacement by transplantation of isolated hepatocytes in rats treated with retrorsine. Am. J. Pathol. 153:319–329; 1998.
9 Lee, K. W.; Lee, J. H.; Shin, S. W.; Kim, S. J.; Joh, J. W.; Lee, D. H.; Kim, J. W.; Park, H. Y.; Lee, S. Y.; Lee, H. H.; Park, J. W.; Kim, S. Y.; Yoon, H. H.; Jung, D. H.; Choe, Y. H.; Lee, S. K. Hepatocyte transplantation for glycogen storage disease type Ib. Cell Transplant. 16: 629–637; 2007.
10. Mito, M.; Ebata, H.; Kusano, M.; Onishi, T.; Hiratsuka, M.; Saito, T. Studies on ectopic liver utilizing hepatocytes transplanted into the rat spleen. Transplant. Proc. 11:585–591; 1979.
11. Mito, M.; Kusano, M. Hepatocyte transplantation in man. Cell Transplant. 2:65–74; 1993.
12. Pertoft, H.; Smedsrød, B. Separation and characterization of liver cells. In: Pretlow, T. G.; Pretlow, T. P., eds. Cell separation, methods and selected applications, vol. 4. New York: Academic Press; 1982:1–24.
13. Sato, H.; Funahashi, M.; Kristensen, B. D.; Tateno, C.; Yoshizato, K. Pleiotrophin as a Swiss 3T3 cell-derived potent mitogen for adult rat hepatocytes. Exp. Cell Res. 246:152–164; 1999.
14. Strom, S. C.; Chowdhury, J. R.; Fox, I. J. Hepatocyte transplantation for the treatment of human disease. Semin. Liver Dis. 19:39–48; 1999.
15. Strom, S. C.; Fisher, R. A.; Rubinstein, W. S.; Barranger, J. A.; Towbin, R. B.; Charron, M.; Mieles, L.; Pisarov, L. A.; Dorko, K.; Thompson, M. T.; Reyes, J. Transplantation of human hepatocytes. Transplant. Proc. 29:2103–2106; 1997.
16. Tanaka, K.; Soto-Gutierrez, A.; Navarro-Alvarez, N.; Rivas-Carrillo, J. D.; Jun, H-S.; Kobayashi, N. Functional hepatocyte culture and its application to cell therapies. Cell Transplant. 15:855–864; 2006.
17. Tateno, C.; Takai-Kajihara, C.; Yamasaki, C.; Sato, H.; Yoshizato, K. Heterogeneity of growth potential of adult rat hepatocytes in vitro. Hepatology 31:65–74; 2000.
18. Tateno, C.; Yoshizato, K. Long-term cultivation of adult rat hepatocytes that undergo multiple cell divisions and express normal parenchymal phenotypes. Am. J. Pathol. 148:383–392; 1996.
19. Tateno, C.; Yoshizato, K. Growth and differentiation in culture of clonogenic hepatocytes that express both phenotypes of hepatocytes and biliary epithelial cells. Am. J. Pathol. 149:1593–1605; 1996.